The Release of Drops of Molten Ferrosilicon and Silicon into Water: Pressure Transients Generated During Triggered Steam Explosions

L.S. Nelson, P.W. Brooks, R. Bonazza,
M.L. Corradini, K. Hildal

November 2004

UWFDM-1230

FUSION TECHNOLOGY INSTITUTE

UNIVERSITY OF WISCONSIN

MADISON WISCONSIN

The Release of Drops of Molten Ferrosilicon and Silicon into Water: Pressure Transients Generated During Triggered Steam Explosions

L.S. Nelson, P.W. Brooks, R. Bonazza, M.L. Corradini, K. Hildal*

Fusion Technology Institute
University of Wisconsin
1500 Engineering Drive
Madison, WI 53706

http://fti.neep.wisc.edu

November 2004

UWFDM-1230

*Institute of Metallurgy, Norwegian University of Science and Technology, N-7491 Trondheim, Norway

ABSTRACT

The experiments described here were directed toward interpreting and understanding pressure-time records generated during triggered steam explosions of single drops of molten silicon and ferrosilicon. These experiments extend the observations of pressurizations produced last year during a triggered explosion of a single drop of molten silicon.

After discussing experimental improvements and the characterization of Impactor 3, we describe new experiments performed with single drops of the molten ferrosilicon alloy (75 wt. % Si, 25 wt. % Fe) and drops of silicon, both nonalloyed and containing small amounts of Al and/or Ca additives.

We obtained new information about the triggered steam explosions of drops of these molten metals primarily from new instrumentation used this year: the transducer-oscilloscope pressure measuring system, a high-speed video system, and a hydrogen collection and measuring system.

Of greatest importance has been the ability to correlate individual video images exactly in time with various characteristics of the pressure-time traces.

INTRODUCTION

During the year 2000, our experiments were devoted primarily to obtaining and interpreting the pressure-time records generated during triggered steam explosions of single drops of molten silicon and ferrosilicon. These experiments extend the observations made during 1999 of the pressure transients produced in one preliminary experiment (D-150-1) in which a single drop of molten silicon was triggered and exploded (Nelson et al., 2000).

Early in 2000 we concentrated mostly on recording pressure transients generated during triggered explosions of single drops of the molten ferrosilicon alloy that contains nominally 75 wt. % silicon and 25 wt. % iron (FeSi75). Later in the year, we turned to recording the transients generated similarly during the triggered explosions of single drops of molten silicon and compared them with the transients produced by the drops of molten ferrosilicon and the triggering pulses used to initiate the explosions. We also examined the effects on these interactions of (a) triggering drops of molten silicon at various depths and (b) of alloying small amounts of Al and Ca with the silicon. At midyear, we borrowed a high-speed video system that provided very valuable information in three important experiments.

EXPERIMENTAL

Preparation of Drops of the Molten Alloys

We began the experiments in year 2000 with the ferrosilicon because its lower melting temperature requires a lower furnace temperature, and thus exposes the silicon carbide heating element to lower risk of failure. (Heating element failure was a major concern in the experiments during 1999; see Appendix C in Nelson et al., 2000).

The ferrosilicon rods were from batch F1/F2 (C-121-1), with composition as shown in Table 1 (the lesser constituents other than Al and Ca have been omitted).

Table 1. Composition of Ferrosilicon Rods Supplied by SINTEF Materials Technology, Trondheim, Norway.

SINTEF No.	UW No.	Si (w/o)	Fe (w/o)	Al (w/o)	Ca (w/o)
F1/F2	C-121-1	73.8	25.1	<0.001	0.001

These rods have the lowest level of impurities of any of the ferrosilicon samples supplied by SINTEF Materials Technology, Trondheim, Norway.

During the year 2000, we also looked further at how the steam explosions are affected by alloying the silicon drops. These experiments repeat similar work performed in 1999 (Nelson et al., 2000), but with the addition of pressure-time measurements during the triggered interactions.

The experiments were performed with drops prepared from rods taken from one of three batches of alloyed silicon used earlier (Nelson et al., 2000). The weight percentages of the major elements alloyed with these rods are shown in Table 2:

Table 2. Major Additive Elements in Three Batches of Alloyed Silicon

Element	Batch B (Wt. %)	Batch C (Wt. %)	Batch D (Wt. %)
Fe	0.028	0.033	0.032
Ca	0.011	0.043	0.032
Al	0.51	0.064	0.57

The complete analyses of these rods are given in Table A-1 of Appendix A.

Furnace

In order to minimize the failures of the silicon carbide furnace elements experienced last year (Nelson et al., 2000), we made two improvements to the furnace: 1) To reduce the current required to reach a given furnace temperature, we installed new, more efficient furnace insulation, ALTRA KVS 18/700, made by Rath Performance Fibers, Inc. It is reportedly usable to temperatures as high as 1800 ^{o}C. 2) To avoid excessive currents, we installed an ammeter in the 110 V AC mains leading to the variable voltage transformer that provides power to the furnace.

Recalibration of the Tourmaline Transducer

Because the main emphasis during year 2000 involved measurement of pressure transients generated by both the triggering source and the steam explosions, we returned the tourmaline underwater blast transducer (Nelson et al., 1999a**)** to its manufacturer, PCB Piezotronics, Depew, NY, for an overall checkup, recalibration and refurbishment. An improved watertight cable was installed, the preamplifier was checked,

PCB PIEZOTRONICS INC.

CALIBRATION CERTIFICATE

Model:	W138A01/038CY020AC	**Date:**	6/19/00
Serial #:	4809	**By:**	Tom Johnston, Cal. Tech.
Description:	Pressure Sensor	**Station:**	Bomb'e Huile
Type:	ICP		
Sensitivity*:	4.714 mV/PSI		
Linearity*:	0.42% FS	**Cert #:**	64864
Bias:	10.8 VDC		

* Zero based, least-squares straight line.

Notes:
1 Calibration is traceable to NIST up to 15,000 psi static and complies with ISO 10012-1 and former MIL-STD-45662A.
2 NIST traceablity through project # 822/255136-95
3 This certificate may not be reproduced, except in full, without written approval.

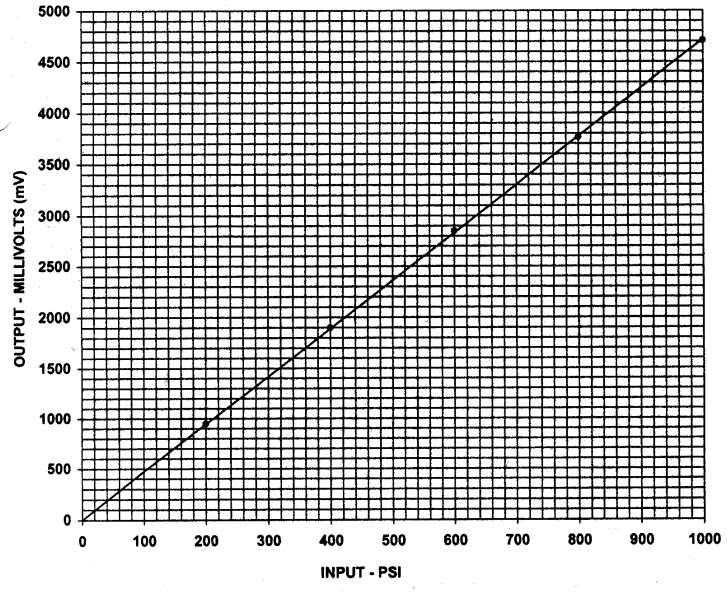

TEST DATA

INPUT (PSI)	OUTPUT (mV)
200	947
400	1897
600	2848
800	3761
1000	4705

PCB PIEZOTRONICS, INC.
3425 Walden Avenue, Depew NY 14043
Tel: 716-684-0001 Fax: 716-684-0987
Email: sales@pcb.com Web: www.pcb.com

ISO 9001 CERTIFIED

Figure 1a. Calibration certificate for the tourmaline underwater blast transducer used in this work, dated 6/19/00.

PCB PIEZOTRONICS

CALIBRATION CERTIFICATE

Model:	W138A01/033CY020AC		
Serial #:	4809	Date:	4/23/98
Description:	Pressure Sensor	By:	Tom Johnston, Cal. Tech.
Type:	ICP	Station:	Bomb'e Huile
Sensitivity:	4.930 mV/PSI		
Linearity:	0.89% FS		
		Cert #:	3164

Notes:

1 Calibration is traceable to NIST up to 15,000 psi static and complies with ISO 10012-1 and former MIL-STD-45662A.
2 Calibration is traceable to NIST and complies with ISO 10012-1 and former MIL-STD-45662A.
3 NIST traceability through project # 822/255136-95
4 This certificate may not be reproduced, except in full, without written approval.

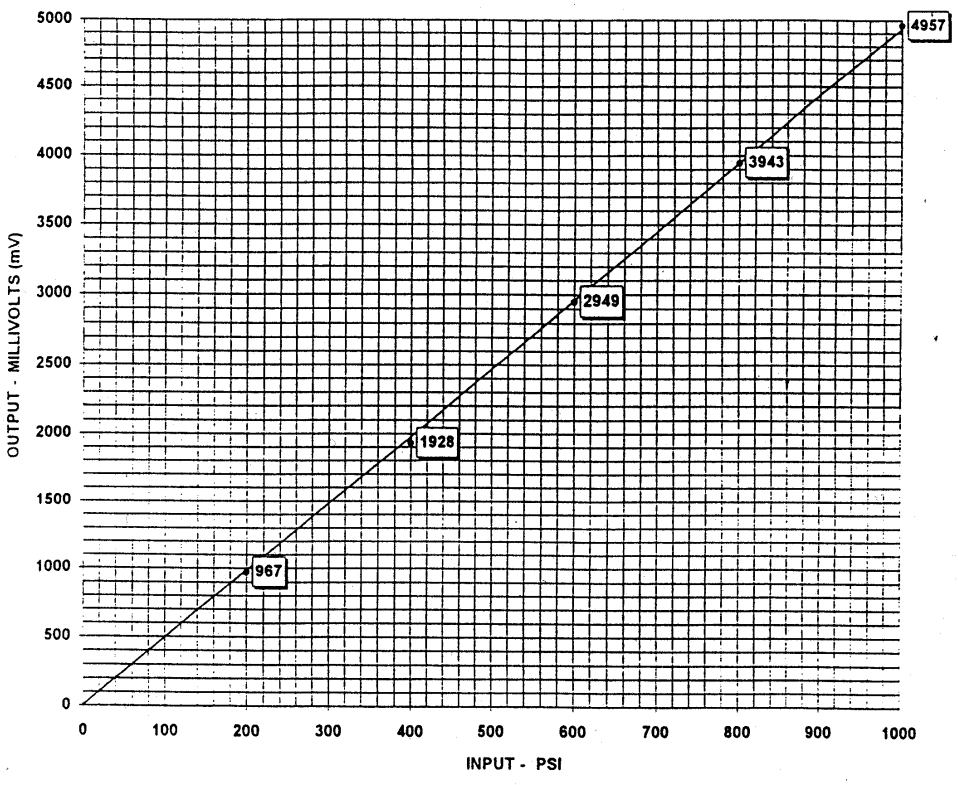

PCB PIEZOTRONICS, INC.
3425 Walden Avenue, Depew NY 14043
Tel: 716-684-0001 Fax: 716-684-0987
Email: sales@pcb.com Web: www.pcb.com

ISO 9001 CERTIFIED

Figure1b. Calibration certificate for the tourmaline underwater blast transducer used in this work, dated 4/23/98.

the battery was replaced, and a new calibration was prepared. The new calibration is shown in Figure 1a, and should be compared to the previous calibration shown in Figure 1b. The new conversion factor for the transducer is 0.683 V/MPa, compared to 0.716 V/MPa, determined in 1998–a decrease in sensitivity of only about 5% after more than two years of use.

Experimental Procedures

The techniques and procedures used during year 2000 for the release of the molten drops, photographic and video imaging, triggering of the interactions, collection and measurement of hydrogen and transducer-oscilloscope recording of the pressure transients generated during the interactions are essentially identical to those reported in previous years (Nelson et al., 1999a, 1999b, 2000). The interactions were triggered with pressure transients generated by Impactor 3 (Nelson et al., 2000). Additionally, during 2000, we were able to use a high-speed video imaging system for several experiments.

We made two modifications during the second half of the year when we switched to drops of molten silicon after studying drops of molten ferrosilicon:

- We increased the furnace temperature from about 1450 ^{o}C to about 1525 ^{o}C to accommodate the higher melting temperature of silicon; and
- We decreased the distance between the drops and Impactor 3 at the time of triggering to produce the stronger pressure transients needed to initiate the explosions of silicon drops.

High-Speed Video System

Thanks to the generosity of the Engine Research Laboratory, University of Wisconsin, we were able to borrow their Kodak Ektapro HS Motion Analyzer, Model 4540, for several days to image steam explosion-related events. This unit will record a total of up to 1024 video frames per run at rates up to 4500 frames per second. To trigger the Ektapro camera, we used a relay closure operated by the 110 V AC signal that fires Impactor 3. Imaging was done in reflected light provided by two banks of three fluorescent tube lamps, one at either side of our water chamber. The images were saved both on standard VHS video tape and also in frame-by-frame digital format on floppy disks. Times and other pertinent data are included in each recorded frame. We photographed a video monitor to record single frames selected from the Ektapro VHS tape.

RESULTS

Overview

Triggered Interactions of Drops of Molten Ferrosilicon and Silicon

In the first half of the year 2000, we performed twelve experiments with drops of the molten ferrosilicon alloy, FeSi75. The experiments are summarized in Tables 3a and 3b, in which the data are presented (a) in the order in which they were performed, and (b) sorted according to the depth of the impactor in the water. Note that eleven experiments were imaged in a darkened room with the camcorder and one or two 35 mm cameras, while the twelfth experiment (D-199-1) was imaged with both the camcorder and the high-speed video camera using reflected light.

In the second half of the year 2000, we performed eleven experiments with drops of the molten silicon. Eight were performed with nonalloyed silicon and are summarized in Tables 4a and 4b; three more experiments were performed with drops of molten silicon that had been alloyed with small amounts of Al and/or Ca and are summarized in Table 5. As with the ferrosilicon drops, all experiments but one were imaged in a darkened room with the camcorder and one or two 35 mm cameras. One experiment (D-202-1) was imaged with both the camcorder and the high-speed video camera using reflected light.

Pressure-Time Traces

We have recorded an extensive series of pressure-time measurements with the tourmaline transducer-oscilloscope combination during or related to the triggered interactions of single drops of the molten ferroalloys with water. This series began with the preliminary experiment D-150-1 in 1999 (see Appendix B in Nelson et al., 2000). During these experiments, at least 100 pressure-time traces with 32,768 data points each have been recorded and saved to floppy disk

Because of the large number of traces and their complexity, it has not been possible to describe and analyze them completely in this report. Therefore, we will concentrate on only a few of these traces here. First, we will discuss those used to characterize the impactor pulses, and later, we will concentrate on those recorded simultaneously with high-speed video imaging; more extensive discussion of the other traces will be reserved for a later time.

Characteristics of Impactor 3

Because Impactor 3 was used as the triggering source throughout these new experiments, it is important to describe its behavior in somewhat greater detail than in our preliminary discussions (Nelson et al., 2000).

Generation of Peak Pressures by Impactor 3

Impactor 3 operates when a 60 g, 15 mm-diameter X 39 mm-tall steel slug is driven upward in a rifle-like barrel by gas at high pressure (1.3 MPa, 185 psi). The pressure transient is generated in the water when the slug strikes the underside of the cover of a welded, watertight carbon steel canister. A typical pressure-time record generated by this impactor when fired in the water at a depth of 400 mm with the tourmaline transducer 100 mm above at a depth of 300 mm is shown in Figure 2 (D-168-1-4).

Note that the trace shows two primary pressurizations, a strong first peak and a lesser peak 2.56 ms later. This pattern of pressurizations is produced whenever the impactor is fired, as discussed previously in relation to experiment D-150-1 (Nelson et al., 2000). As before, we label these two transients PT 1 and PT 2.

Initially, we shall characterize these pulses by their maximum values–the peak pressures–the most easily measured parameter.

Table 3a. Summary of Release of 9 mm-Diameter Drops of Nonalloyed Molten Ferroslicon into Water.
Interaction was triggered with Impactor 3; air pressure was 1.3 Mpa. In order of performance.
In each experiment, the silicon rod was supported in the furnace on a graphite cross-rod.

Drop No.	Alloy	T(water) (°C)	T(furnace) (°C)	Furnace Atm.	Rod Loss Wt (g)	Debris Wt. (g)	Difference (g)	Depths (mm) Impactor	Depths (mm) Photodet'r	Delay (s)	Trigger[a] (mm)	Trigger[b] (Mpa)	Imaging	$V(H_2)$ (ml)	Remarks
D-163-1	F1/F2	22	1475	Ar + 1%H_2	1.17, 1.18	0.89	0.29	500	400	0	70	2.44	OS, VCR	NM	Good explosion; H_2 collector
	(C-121-1)				Total 2.35										failed, scope showed only noise.
D-168-1	F1/F2	22.8	1426	Ar + 1%H_2	1.19	0.9	0.29	400	300	0	60	2.85	OS, VCR	4.8	Good explosion. Everything
	(C-121-1)														worked. P trace shows 2 peaks
															from collapse of 2 bubbles .
D-170-1	F1/F2	23.6	1435	Ar + 1%H_2	1.16	1.07	0.09	600	500	0	70	2.44	OS, VCR	2.0	Moderate explosion. Everything
	(C-121-1)														worked. P trace shows 2 extra
															peaks.
D-173-1	F1/F2	24.3	1440	Ar + 1%H_2	1.17	1.03	0.14	820	720	0	55	3.11	OS, VCR	1.0	Scope trace of explosion not
	(C-121-1)														saved; photo only.
D-175-1	F1/F2	24.4	1420	Ar + 1%H_2	1.13	0.99	0.14	500	400	0	70	2.44	OS, VCR	1.3	Scope showed only noise; poor
	(C-121-1)						Lost 12%						2 cameras		triggering.
D-178-1	F1/F2	20.7	1440	Ar + 1%H_2	1.22	1.14	0.08	500	400	0	75	2.28	OS, VCR	0.6	Mild esplosion, some chunks
	(C-121-1)						Lost 7%						2 cameras		afterward. Good scope traces
															with extra peaks. Drop hit cone
															on entering the water.
D-180-1	F1/F2	23.0	1450	Ar + 1%H_2	1.20, 1.12	0.96	0.16	500	400	0	60	2.85	OS, VCR	1.3	1st drop swerved right, fell
	(C-121-1)				Total 2.32		Lost 14 %						2 cameras		beneath pan; 2nd exploded
															strongly.Good photos and scope
															trace with extra peaks.
D-182-1	F1/F2	23.3	1470	Ar + 1%H_2	1.48	1.27	0.21	355	255	0	70	2.44	OS, VCR	2.2	Strong explosion; good pressure
	(C-121-1)						Lost 14 %						2 cameras		trace and photos.
D-184-1	F1/F2	23.4	1455	Ar + 1%H_2	1.53	1.55	0.02	465	300	0	90	1.90	OS, VCR	0.2	Decreased trigger by about 50 %.
	(C-121-1)						Gain 1 %						2 cameras		Mild interaction thatblew out top
															of drop. Pressure trace similar
															to impactor.
D-187-1	F1/F2	23.2	1460	Ar + 1%H_2	1.47	1.18	0.29	435	300	0	100	1.71	OS, VCR	3.1	The most vigorous FeSi explosion
	(C-121-1)						Lost 20 %						2 cameras		of the series so far.Threw water.
															Huge pressure spike.
D-188-1	F1/F2	22.8	1440	Ar + 1%H_2	1.49	1.33	0.16	270	193	0	50	3.42	OS, VCR	>4.2	Shallowest impactor depth.
	(C-121-1)						Lost 11 %						2 cameras		Transducer is horizontal. Very
															large pressure spike. May have
															lost some hydrogen.
D-199-1	F1/F2	24.3	1440	Ar + 1%H_2	1.23	1.05	0.18	355	255	0	80	2.14	EKTAPRO	44.6	Good explosion, video images at
	(C-121-1)						Lost 15 %						RL, VCR		4500 & 60 f/s; strong pressure
															trace.

[a] This is the distance above the impactor at which the drop was exposed to the triggering pulse. It was estimated from the video and photographic images.

[b] This value was calculated from the distance above the impactor and the peak pressure generated by the impactor of 1.71 Mpa, measured at 100 mm (see Figure 3), using the 1/r relationship.

Table 3b. Summary of Release of 9 mm-Diameter Drops of Nonalloyed Molten Ferroslicon into Water.
Interaction was triggered with Impactor 3; air pressure was 1.3 Mpa. Sorted by impactor depth.
In each experiment, the silicon rod was supported in the furnace on a graphite cross-rod.

		T(water)	T(furnace)	Furnace	Rod Loss	Debris	Difference	Depths (mm)		Delay	Trigger[a]	Trigger[b]			
Drop No.	Alloy	(°C)	(°C)	Atm.	Wt (g)	Wt. (g)	(g)	Impactor	Photodet'r	(s)	(mm)	(Mpa)	Imaging	$V(H_2)$ (ml)	Remarks
D-188-1	F1/F2	22.8	1440	Ar + 1%H_2	1.49	1.33	0.16	270	193	0	50	3.42	OS, VCR	>4.2	Shallowest impactor depth.
	(C-121-1)						Lost 11 %						2 cameras		Transducer is horizontal. Very large pressure spike. May have lost some hydrogen.
D-182-1	F1/F2	23.3	1470	Ar + 1%H_2	1.48	1.27	0.21	355	255	0	70	2.44	OS, VCR	2.2	Strong explosion; good pressure
	(C-121-1)						Lost 14 %						2 cameras		trace and photos.
D-199-1	F1/F2	24.3	1440	Ar + 1%H_2	1.23	1.05	0.18	355	255	0	80	2.14	EKTAPRO	44.6	Good explosion, video images at
	(C-121-1)						Lost 15 %						RL, VCR		4500 & 60 f/s; strong pressure trace.
D-168-1	F1/F2	22.8	1426	Ar + 1%H_2	1.19	0.9	0.29	400	300	0	60	2.85	OS, VCR	4.8	Good explosion. Everything
	(C-121-1)														worked. P trace shows 2 peaks from collapse of 2 bubbles .
D-187-1	F1/F2	23.2	1460	Ar + 1%H_2	1.47	1.18	0.29	435	300	0	100	1.71	OS, VCR	3.1	The most vigorous FeSi explosion
	(C-121-1)						Lost 20 %						2 cameras		of the series so far.Threw water. Huge pressure spike.
D-184-1	F1/F2	23.4	1455	Ar + 1%H_2	1.53	1.55	0.02	465	300	0	90	1.90	OS, VCR	0.2	Decreased trigger by about 50 %.
	(C-121-1)						Gain 1 %						2 cameras		Mild interaction thatblew out top of drop. Pressure trace similar to impactor.
D-163-1	F1/F2	22	1475	Ar + 1%H_2	1.17, 1.18	0.89	0.29	500	400	0	70	2.44	OS, VCR	NM	Good explosion; H_2 collector
	(C-121-1)				Total 2.35										failed, scope showed only noise.
D-175-1	F1/F2	24.4	1420	Ar + 1%H_2	1.13	0.99	0.14	500	400	0	70	2.44	OS, VCR	1.3	Scope showed only noise; poor
	(C-121-1)						Lost 12%						2 cameras		triggering.
D-178-1	F1/F2	20.7	1440	Ar + 1%H_2	1.22	1.14	0.08	500	400	0	75	2.28	OS, VCR	0.6	Mild esplosion, some chunks
	(C-121-1)						Lost 7%						2 cameras		afterward. Good scope traces with extra peaks. Drop hit cone on entering the water.
D-180-1	F1/F2	23.0	1450	Ar + 1%H_2	1.20, 1.12	0.96	0.16	500	400	0	60	2.85	OS, VCR	1.3	1st drop swerved right, fell
	(C-121-1)				Total 2.32		Lost 14 %						2 cameras		beneath pan; 2nd exploded strongly.Good photos and scope trace with extra peaks.
D-170-1	F1/F2	23.6	1435	Ar + 1%H_2	1.16	1.07	0.09	600	500	0	70	2.44	OS, VCR	2.0	Moderate explosion. Everything
	(C-121-1)														worked. Pressure trace shows two extra peaks.
D-173-1	F1/F2	24.3	1440	Ar + 1%H_2	1.17	1.03	0.14	820	720	0	55	3.11	OS, VCR	1.0	Scope trace of explosion not
	(C-121-1)														saved; photo only.

[a] This is the distance above the impactor at which the drop was exposed to the triggering pulse. It was estimated from the video and photographic images.

[b] This value was calculated from the distance above the impactor and the peak pressure generated by the impactor of 1.71 Mpa, measured at 100 mm (see Figure 3), using the 1/r relationship.

Table 4a. Summary of Release of 9 mm-Diameter Drops of Nonalloyed Molten Silicon into Water[a]
Interaction was triggered with Impactor 3; air pressure was 1.3 Mpa. In order of performance.
In each experiment, the silicon rod was supported in the furnace on a graphite cross-rod.

								Depths (mm)							
Drop No.	Alloy	T(water) (°C)	T(furnace) (°C)	Furnace Atm.	Rod Loss Wt (g)	Debris Wt. (g)	Difference (g)	Impactor	Photodet'r	Delay (s)	Trigger[a] (mm)	Trigger[b] (Mpa)	Imaging	$V(H_2)$ (ml)	Remarks
D-191-2	A-5	24.0	1520	Ar + 1%H_2	1.15	1.15	0.00	400	300	0	310	1.9	OS, VCR	2.0	Impactor triggered but no
													2 Cameras		explosion. Scope showed only
															impactor trace. Blown out
															globule was recovered.
D-194-1	A-5	23.3	1520	Ar + 1%H_2	0.85	0.83	0.02	400	335	0	no picture	NM	OS, VCR	NM	Drop fell behind the impactor; no
							Lost 2.3%						2 Cameras		explosion. Scope showed only
															impactor trace.Blown out globule.
D-197-1	A-5	23.4	1520	Ar + 1%H_2	2.55	2.55	0.00	400	350	0	365	4.9	OS, VCR	#1, 3.4	Drop #1 fell on blinder
					2 drops								2 Cameras	#2, 6.5	untriggered; drop #2 triggered but
															only fragmented coarsely.
D-202-1	A-5	24.4	1520	Ar + 1%H_2	1.21	0.86	0.35	355	305	0	305	3.4	EKTAPRO	NM. Too	Very strong explosion; threw
							Lost 29%						VCR in RL	violent	water. Good high-speed images.
															Very large spike on scope. Fine
															debris plus a few chunks.
D-205-1	A-5	NM	1520	Ar + 1%H_2	1.00	0.88	0.12	355	305	0	305	3.4	OS, VCR	2.5	Strange mild explosion; spherical
							Lost 12%						2 Cameras		on photos but only 1st pulse from
															impactor on scope. Chunks plus
															fines.
D-207-1	A-5	23.8	1520	Ar + 1%H_2	1.05	0.86	0.19	350	300	0	310	4.3	OS, VCR	1.8	Excellent explosion, far forward.
							Lost 18%						2 Cameras		Spherical on photos. Lost scope
															trace. Chunks plus fines.
D-209-1	A-5	23.6	1520	Ar + 1%H_2	1.28	0.97	0.31	360	310	0	325	4.9	OS, VCR	3.3	Drop hit blinder, then fell and
							Lost 24%						2 Cameras		exploded at left; spherical on
															photos. Small spike on scope
															trace. Chunks plus fines.
D-214-1	A-5	21.9	1525	Ar + 1%H_2	1.33	1.55	0.18	200	150	0	150	3.4	OS, VCR	NM	Fresh water. No H_2 collector.
							Lost 14 %						2 Cameras		Moderate explosion plus burning
															particles. Unusual scope trace.
															Chunksand fines.
D-223-1	A-5	23.2	1535	Ar + 1%H_2	1.23	1.01	0.22	300	260	0	260	4.3	OS, VCR	4.0	Strong explosion; PT 2= PT !;
							Lost 18 %								eggshells and fines.

[a] This is the distance above the impactor at which the drop was exposed to the triggering pulse. It was estimated from the video and photographic images.

[b] This value was calculated from the distance above the impactor and the peak pressure generated by the impactor of 1.71 Mpa, measured at 100 mm (see Figure 3), using the 1/r relationship.

Table 4b. Summary of Release of 9 mm-Diameter Drops of Nonalloyed Molten Slicon into Water[a]
Interaction was triggered with Impactor 3; air pressure was 1.3 Mpa. Sorted by impactor depth.
In each experiment, the silicon rod was supported in the furnace on a graphite cross-rod.

Drop No.	Alloy	T(water) (°C)	T(furnace) (°C)	Furnace Atm.	Rod Loss Wt (g)	Debris Wt. (g)	Difference (g)	Depths (mm) Impactor	Depths (mm) Photodet'r	Delay (s)	Trigger[b] (mm)	Trigger[b] (Mpa)	Imaging	$V(H_2)$ (ml)	Remarks
D-214-1	A-5	21.9	1525	Ar + 1%H_2	1.33	1.55	0.18	200	150	0	150	3.4	OS, VCR	NM	Fresh water. No H_2 collector.
							Lost 14 %						2 Cameras		Moderate explosion plus burning particles. Unusual scope trace. Chunksand fines.
D-223-1	A-5	23.2	1535	Ar + 1%H_2	1.23	1.01	0.22	300	260	0	260	4.3	OS, VCR	4.0	Strong explosion; PT 2= PT !;
							Lost 18 %								eggshells and fines.
D-207-1	A-5	23.8	1520	Ar + 1%H_2	1.05	0.86	0.19	350	300	0	310	4.3	OS, VCR	1.8	Excellent explosion, far forward.
							Lost 18%						2 Cameras		Spherical on photos. Lost scope trace. Chunks plus fines.
D-202-1	A-5	24.4	1520	Ar + 1%H_2	1.21	0.86	0.35	355	305	0	305	3.4	EKTAPRO	NM. Too	Very strong explosion; threw
							Lost 29%						VCR in RL	violent	water. Good high-speed images. Very large spike on scope. Fine debris plus a few chunks.
D-205-1	A-5	NM	1520	Ar + 1%H_2	1.00	0.88	0.12	355	305	0	305	3.4	OS, VCR	2.5	Strange mild explosion; spherical
							Lost 12%						2 Cameras		on photos but only 1st pulse from impactor on scope. Chunks plus fines.
D-209-1	A-5	23.6	1520	Ar + 1%H_2	1.28	0.97	0.31	360	310	0	325	4.9	OS, VCR	3.3	Drop hit blinder, then fell and
							Lost 24%						2 Cameras		exploded at left; spherical on photos. Small spike on scope trace. Chunks plus fines.
D-191-2	A-5	24.0	1520	Ar + 1%H_2	1.15	1.15	0.00	400	300	0	310	1.9	OS, VCR	2.0	Impactor triggered but no
													2 Cameras		explosion. Scope showed only impactor trace. Blown out globule was recovered.
D-194-1	A-5	23.3	1520	Ar + 1%H_2	0.85	0.83	0.02	400	335	0	no picture	NM	OS, VCR	NM	Drop fell behind the impactor; no
							Lost 2.3%						2 Cameras		explosion. Scope showed only impactor trace.Blown out globule.
D-197-1	A-5	23.4	1520	Ar + 1%H_2	2.55	2.55	0.00	400	350	0	365	4.9	OS, VCR	#1, 3.4	Drop #1 fell on blinder
					2 drops								2 Cameras	#2, 6.5	untriggered; drop #2 triggered but only fragmented coarsely.

[a] This is the distance above the impactor at which the drop was exposed to the triggering pulse. It was estimated from the video and photographic images.

[b] This value was calculated from the distance above the impactor and the peak pressure generated by the impactor of 1.71 Mpa, measured at 100 mm (see Figure 3), using the 1/r relationship.

Table 5. Summary of Release of 9 mm-Diameter Drops of Alloyed Molten Slicon into Water
Interaction was triggered with Impactor 3; air pressure was 1.3 Mpa.
In each experiment, the silicon rod was supported in the furnace on a graphite cross-rod.

Drop No.	Alloy	T(water) (°C)	T(furnace) (°C)	Furnace Atm.	Rod Loss Wt (g)	Debris Wt. (g)	Difference (g)	Depths (mm) Impactor	Depths (mm) Photodet'r	Delay (s)	Trigger[a] (mm)	Trigger[b] (Mpa)	Imaging	$V(H_2)$ (ml)	Remarks
D-217-1	B	23	1525	Ar + 1%H_2	1.45	1.16	0.29	300	260	0	285	11.3	OS, VCR	NM, Too	Very vigorous explosion, threw
							Lost 20 %						2 Cameras	violent	H_2O; H_2 collector disabled;
															PT 2 > PT1, PT 3 and 4 late;
															very fine debris; very large bubble
D-219-1	C	23.1	1525	Ar + 1%H_2	1.27	1.21	0.06	300	260	0	275	6.8	OS, VCR	3.3	Coarse fragmentation. All debris
							Lost 5 %						2 Cameras		from melt; no flakes. Only PT 1
															with little afterward.
D-221-1	D	21.8	1520	Ar + 1%H_2	1.31	1.31	0	300	260	0	275	6.8	OS, VCR	8.0	Mild interaction with coarse
							No Loss						2 Cameras		fragmentation. Lots ofhydrogen.
															A few flakes. Only PT 1 with little
															afterward.
D-223-1[c]	A-5	23.2	1535	Ar + 1%H_2	1.23	1.01	0.22	300	260	0	260	4.3	OS, VCR	4.0	Strong explosion; PT 2= PT !;
									Lost 18 %				2 Cameras		eggshells & fines.

[a] This is the distance above the impactor at which the drop was exposed to the triggering pulse. It was estimated from the video and photographic images.

[b] This value was calculated from the distance above the impactor and the peak pressure generated by the impactor of 1.71 Mpa, measured at 100 mm (see Figure 3), using the 1/r relationship.

[c] This experiment was performed with a drop of nonaaloyed silicon exposed to triggering conditions identical to the other experiments described in this table.

This experiment was also included in Table 1.

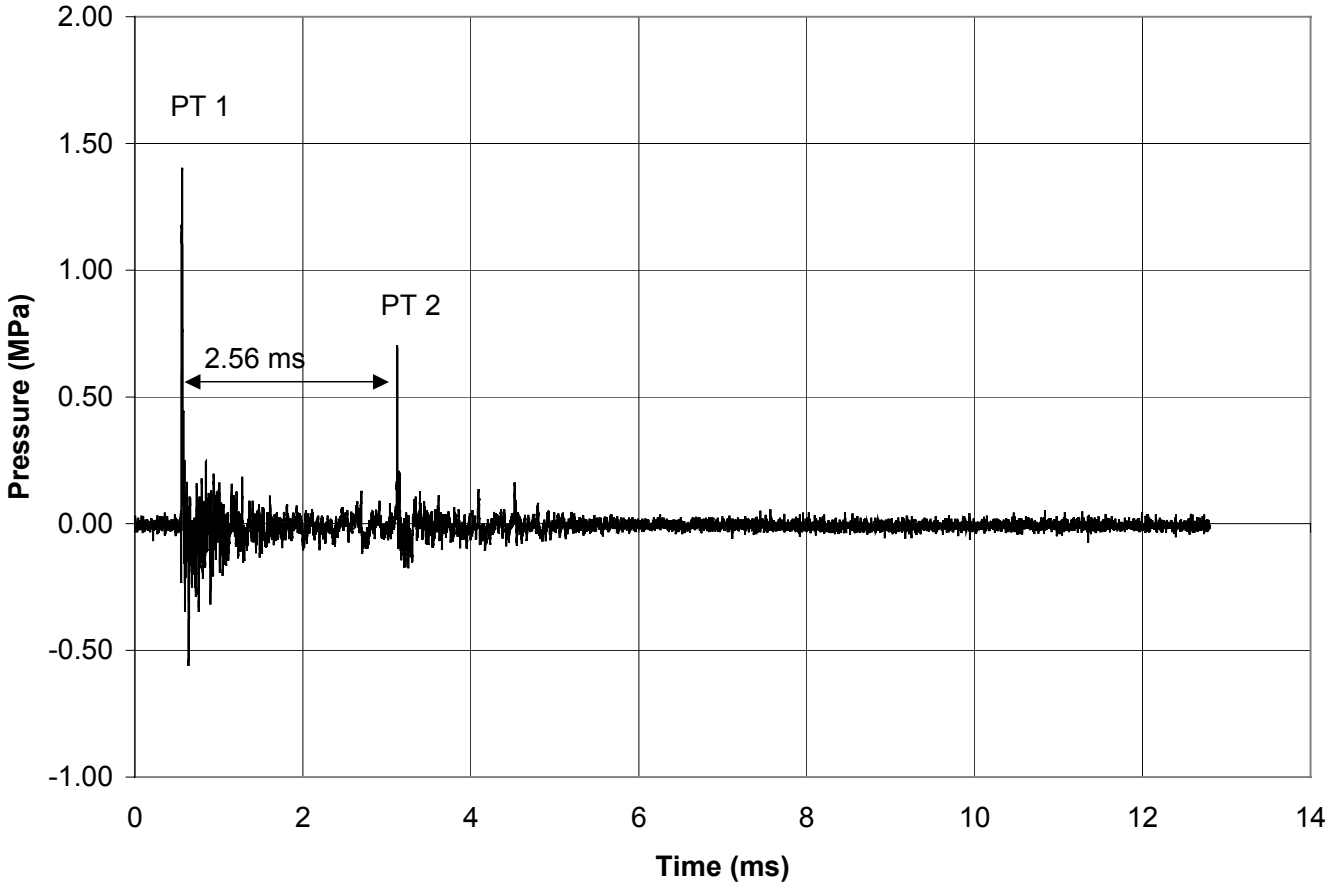

Figure 2. Typical pressure-time record generated by Impactor 3 when fired in water at a depth of 400 mm with the tourmaline transducer 100 mm above at a depth of 300 mm. (D-168-1-4).

Testing Impactor 3

We checked Impactor 3 several times for reproducibility of peak pressures PT 1. The results of typical runs one day apart are shown in Figure 3 (Experiments D-166-2, 167-1). As in Figure 2, the impactor was fired in the water at a depth of 400 mm with the tourmaline transducer 100 mm above at a depth of 300 mm. Both the reproducibility and the repeatability from day to day seemed satisfactory: averages, 1.694 ± 0.069 MPa (±4%) and 1.717 ± 0.04377 MPa (±3%) one day later.

Fine Structure of Pressure Transient PT 1

In Figure 4, we show the fine structure in the transient PT 1, by enlarging the first part of Figure 2 time-wise. Three major pressurizations appear, which we denote as A, B and C. We now attempt to analyze the separations between pairs of these spikes.

Separation A-C

In Figure 4, we show the separation of peaks A and C to be 0.440 ms. We now assume peak C to correspond to the return of a wave reflected from the water surface, a distance of 600 mm (twice that from the transducer to the water surface). Using the speed of sound in water of 1490 m/s, in 0.440 ms the

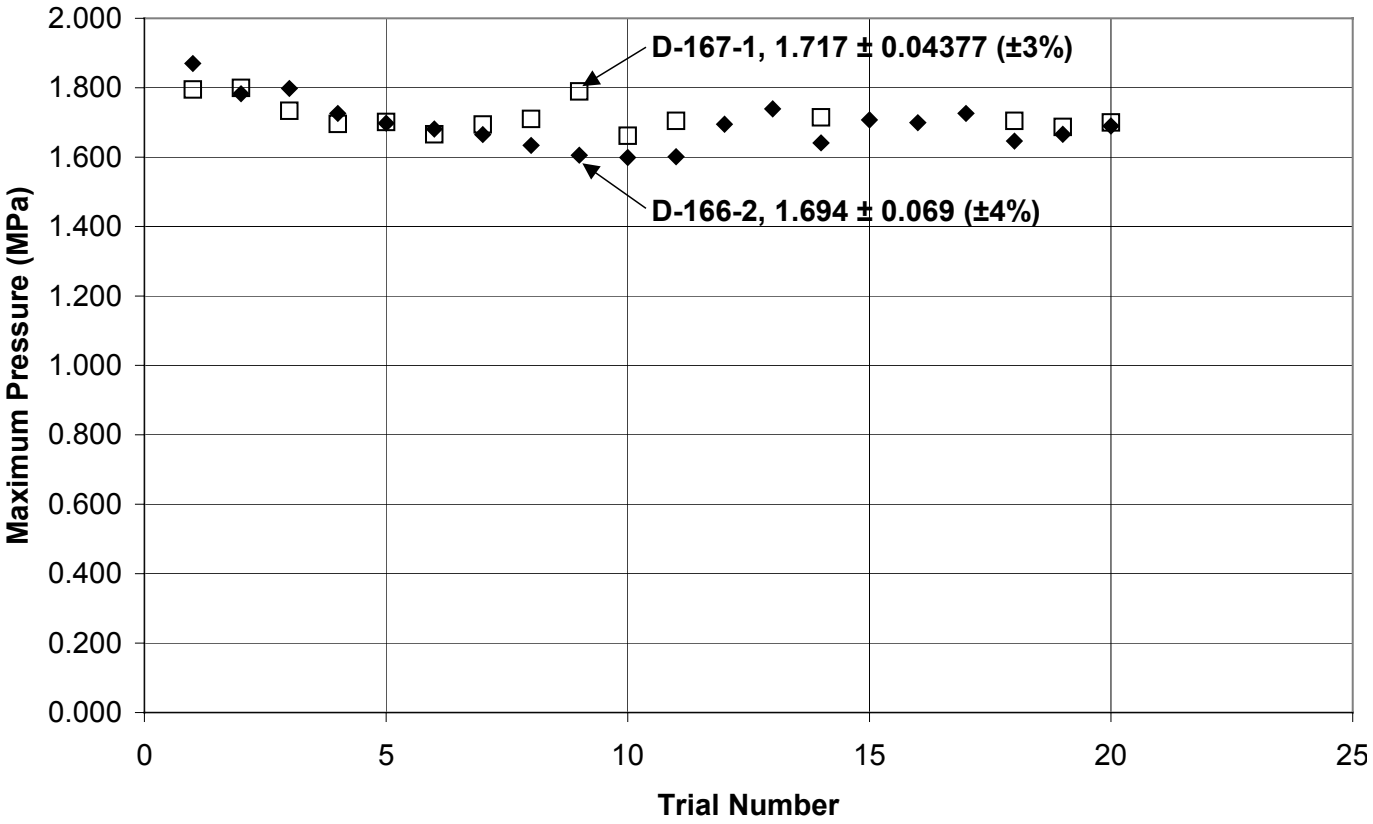

Figure 3. The results of typical firings of Impactor 3 one day apart. As in Figure 2, the impactor was fired in the water at a depth of 400 mm with the tourmaline transducer 100 mm above at a depth of 300 mm.

pressure transient will travel 656 mm. The round trip distance from the transducer to the water surface is 600 mm.

Thus, we believe peak C corresponds to the return of the pressure transient reflected from the surface of the water.

To confirm this identification, we performed another experiment, D-161-2-3, in which the impactor and transducer were both lowered in the water by 100 mm. Now, the round trip distance from the transducer to the water surface is 800 mm. In the new experiment, the separation between peak A and peak C increased from 0.440 ms to 0.579 ms. Again applying the speed of sound in water of 1490 m/s, the travel distance is now estimated to be 862 mm. This is in good agreement with the measured round trip travel of 800 mm from transducer to the water surface and return, and seems to confirm our identification of peak C as being produced by the reflection of the pressure transient from the surface of the water.

Separation A-B

The initial pressurization in PT 1 is actually double-peaked, as shown in both Figures 4 and 5; these peaks have been labeled A and B. (Similar configurations appear in all traces produced with both the pneumatic piston-driven Impactor 2, and the slug-type Impactor 3.) We can apply a procedure similar to that used in the previous section with peaks A and C to identify peak B.

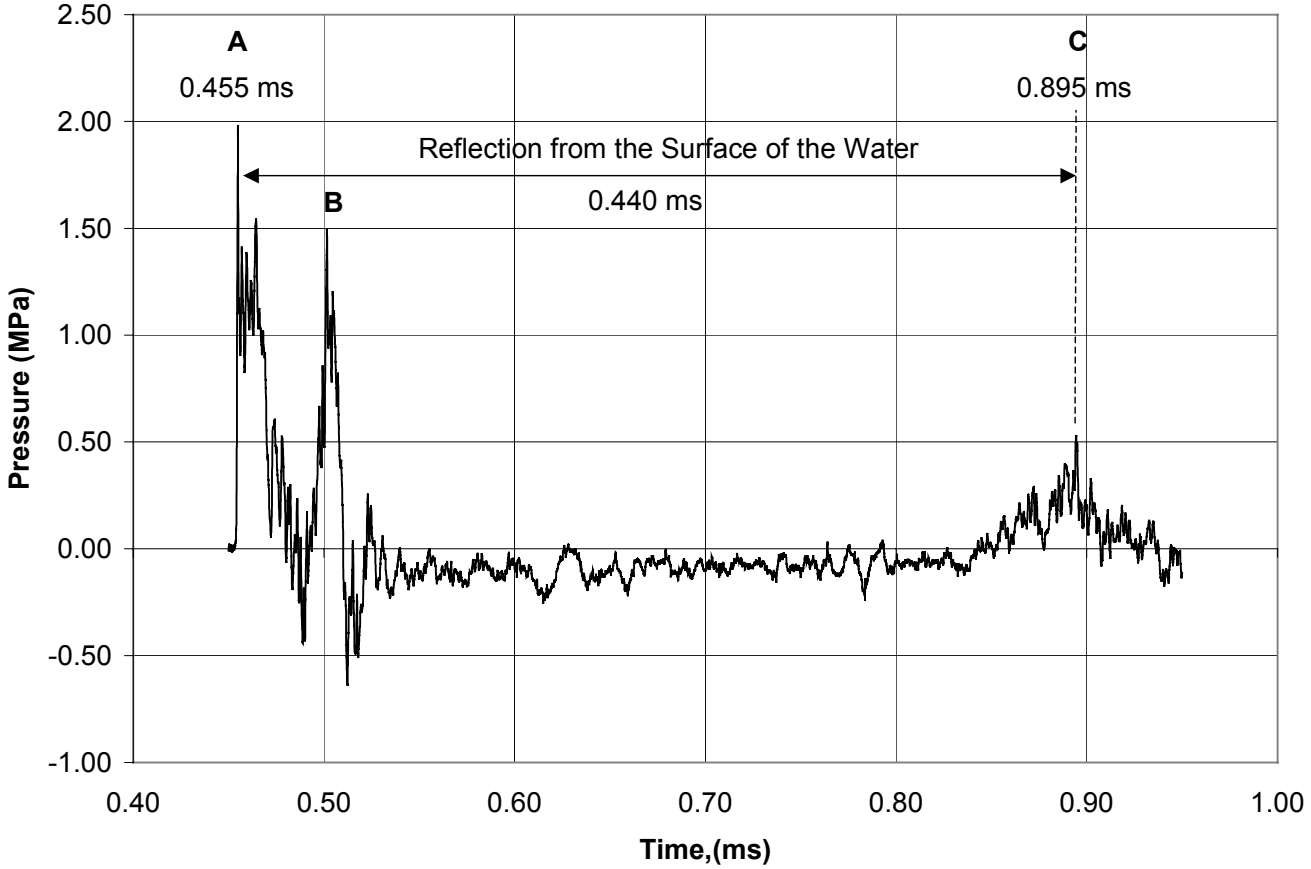

Figure 4. The fine structure in the pressure transient PT 1, shown by enlarging the first part of Figure 2 time-wise (D-168-1-4)..

Now we find the separation between these peaks in Figure 5 to be 0.047 ms. Here we assume peak B to correspond to the return of a wave that passes downward from the surface of the impactor through the steel canister and is reflected from the base of the impactor, a round trip distance of 266 mm (see Figure 1 in Nelson et al., 2000). Using the speed of sound in steel of 5060 m/s, in 0.047 ms the pressure transient will travel 238 mm, again in good agreement with the known dimensions of the canister.

Interpretation of Pressure Transient PT 2

As shown in Figure 2, there are two major peaks generated by the impactor when fired alone. The first, PT 1, has been shown to be caused by the impact of the steel slug against the underside of the canister in which it is enclosed plus secondary reflections of acoustic waves from the base plate of the impactor or from the water surface above.

As shown in Figure 2, there is a second major peak consistently generated by Impactor 3 alone that occurs reproducibly 2.56 ms after the first peak, PT 1. We label this PT 2. By imaging with the Ektapro HS Motion Analyzer at 4500 frames/second, we learned that the second major peak, PT 2, coincides exactly with the secondary diaphragm-like flexure of the upper plate of the impactor. We attribute this pressure peak to a "drumhead-effect" of the impactor. When an elastic surface is struck, the surface will not only swing back to its original position, but also pass the equilibrium point because the surface is not rigid. After the surface reaches its maximum negative position, it will swing back, and this motion results in a second pressure peak. This time it will more or less end its motion at the equilibrium point; that is, both the pressure recordings and high-speed video images show no signs of further motion.

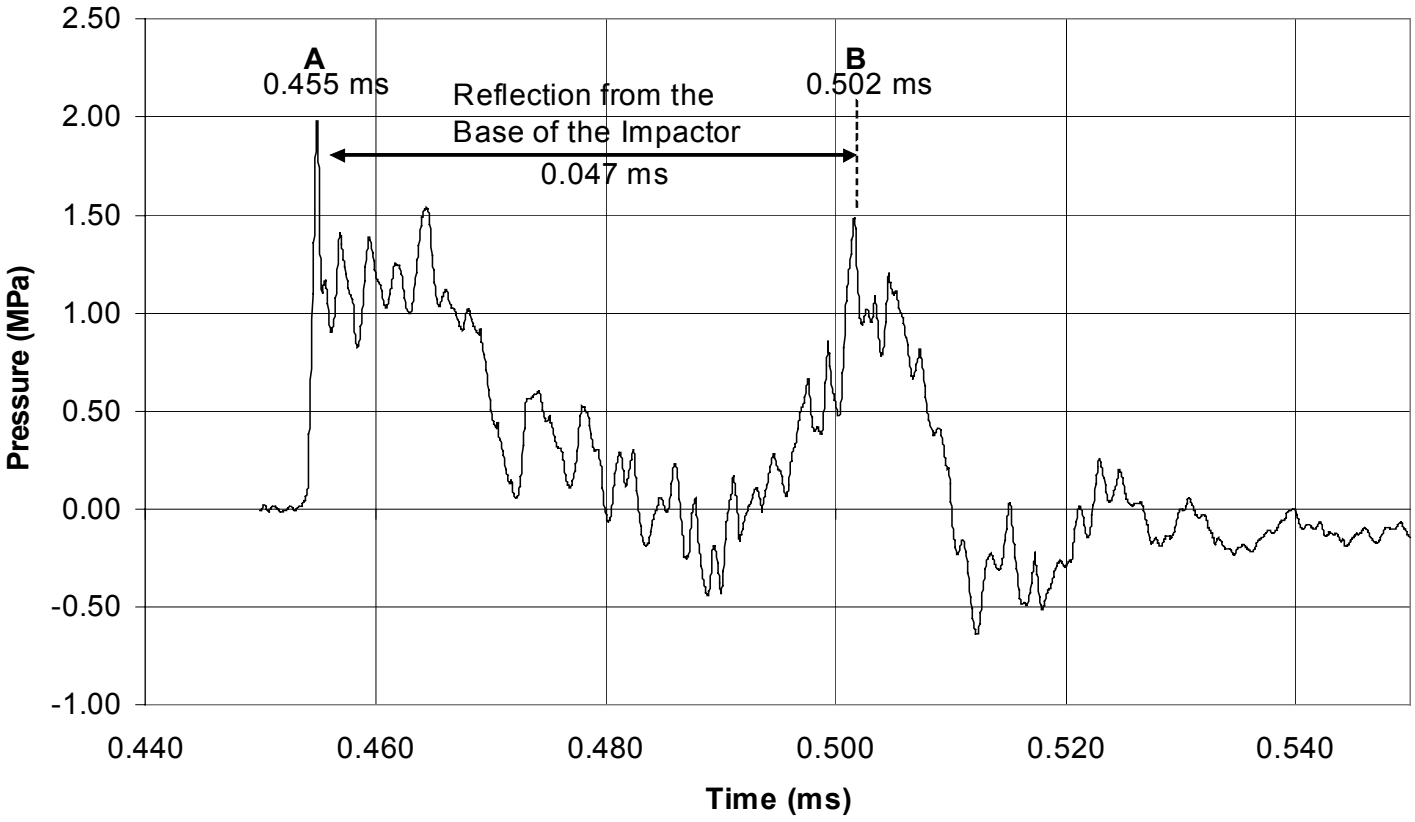

Figure 5. The fine structure in the pressure transient PT 1, shown by further enlarging the first part of Figure 2 time-wise.

Identification of the Peaks–Summary

In summary, then, we have used the speeds of sound in water and steel to identify the three components of pressure transient PT 1 generated by Impactor 3 as follows:

Peak PT 1A. The primary pressurization generated by impact of the steel slug against the underside of the steel top plate the canister.

Peak PT 1B. A secondary pressurization generated by the reflection of the initial pressurization from the base and return to the upper plate of the impactor.

Peak PT 1C. A secondary pressurization generated by the reflection of the initial pressurization from the water surface. This identification has been confirmed by varying the depth of the impactor.

The second major peak, PT 2, coincides exactly with the drumhead-like flexure of the upper plate of the impactor 2.56 ms after the slug strikes the upper plate of the impactor.

Impulses of the Triggering Transients

As we began to experiment with drops of molten FeSi75, we recognized that it is important to distinguish the pressure transients created by the mechanical impactor from the pressure transients created by a violent molten metal-water interaction. The experimental procedure is to record three separate pressure traces, using only the impactor. The impactor can be triggered by shining a flashlight into the photodetector that usually is set off by the bright light of the molten drop. These three recordings are then compared to the recording of the explosion, and we will see that pressure peaks resulting from the impactor are easily distinguished from the explosion pressure peaks. We also found that the impactor gives highly reproducible trigger pressure transients. A good measure for this is the impulse associated with each pressure peak. This is found by integrating the time-pressure curve with respect to time.

It was found that the trigger-impulse was always in the 0.018-0.022 [kPa*s] range, for all the experiments. For each individual experiment, the accuracy was even better. This can be attributed to the fact that the position of the pressure transducer does not change when inserted in the water. Due to transport in and out of the water tank, the position may change slightly between each experiment. In Table 6, we list all the measured impulses resulting from the impactor trigger pulses.

Table 6. Trigger Impulses from the Mechanical Impactor 3**.**

Experiment No.	Trial 1, [kPa*s]	Trial 2, [kPa*s]	Trial 3, [kPa*s]	Trial 4[a] [kPa*s]
D-170-1[b]	0.0212	0.0209	0.0208	0.0209
D-178-1[b]	0.0188	0.0192	0.0195	0.0176
D-180-1[b]	0.0192	0.0198	0.0198	0.0200
D-182-1[b]	0.0190	0.0193	0.0199	0.0187
D-184-1[b]	0.0201	0.0200	0.0198	0.0203
D-187-1[b]	0.0199	0.0203	0.0202	0.0203
D-188-1[b]	0.0215	0.0214	0.0215	0.0206
D-199-1[b]	0.0221	0.0220	0.0223	0.0211
D-202-1[c]	0.0193	0.0197	0.0197	0.0197
D-205-1[c]	missing	0.0195	0.0191	0.0197

[a]Note that Trial 4 is the actual experiment. In case there is a difference between the first three impulses and the last, this is likely to be due to a shielding effect of the drop as it enters the region between the impactor and the transducer.
[b]These experiments were performed with drops of molten ferrosilicon.
[c]These experiments were performed with drops of molten silicon.

By comparing different pressure recordings, we can also see that the shape of the trigger pulse changes very little for each run. A typical trigger pulse has been shown in Figure 2 (see also Figures 4 and 5). There is a quick rise to the peak value; this peak is sometimes but not always preceded by a small, rapid decrease in pressure. Then there is much noise after the initial trigger pressure transient; this is believed to be caused by reflections from the water surface, or from the different structures surrounding the impactor. These disturbances show familiar form and amplitude, and it is not expected that they will have any influence on the interaction between molten metal and water.

To sum up, we found that the pressure trace resulting from firing the impactor is highly reproducible. A good indicator for this is the consistency in the impulses associated with the pressure-time curves. Thus, by determining their impulses, it should be possible to identify pressure transients originating from other sources than the impactor, e.g., a steam explosion.

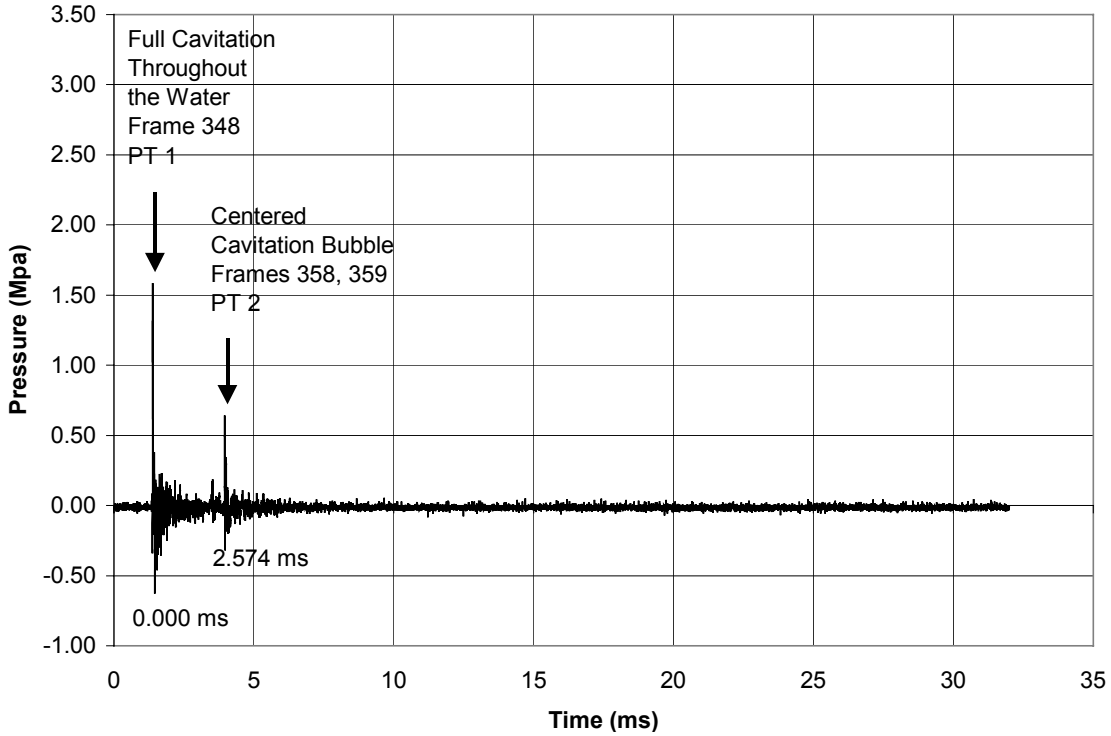

Figure 6. Pressure-time trace generated by Impactor 3 alone in experiment with high-speed video imaging. (D-204-1-4).

Pressure-Time Traces Recorded During High-Speed Video Imaging

During the year 2000, we performed three experiments with high-speed Ektapro video imaging of the interactions: D-199-1-4, with a drop of molten ferrosilicon, FeSi75; D-202-1-4, with a drop of molten non-alloyed silicon; and D-204-1-4, with Impactor 3 fired alone. Pressure-time traces were also recorded during these experiments.

These experiments produced important new information about both the triggering transients and the steam explosions of drops of molten silicon and the molten ferrosilicon alloy FeSi75. This knowledge has been obtained primarily from the ability to identify prominent features in these pressure transients exactly in time with individual video images. In the following sections, we shall attempt to interpret the three traces in terms of selected images reproduced from the high-speed video records.

The Baseline: Impactor 3 Fired Alone (D-204-1-4).

The pressure-time trace generated by firing Impactor 3 alone in experiment D-204-1-4 is shown in Figure 6. This trace is essentially identical to earlier traces generated by Impactor 3 fired alone, for example, those shown as (i) Figure B-3b of Nelson et al., (2000), part of our preliminary experiment, D-150-1, performed in 1999, in which we first measured pressure transients generated during a steam explosion, and (ii) as Figure 2 of this report, recorded in experiment D-168-1-4. It can be seen that these traces are very reproducible and each shows two major peaks 2.6 ms apart that have been designated PT 1 and PT 2 in the earlier reports. Because of this consistency, we can, with confidence, designate these as baseline traces.
By photographing a video monitor, we have recorded a number of individual high-speed images from the Ektapro VHS tape produced during experiment D-204-1-4. In Table 7, we have described these photographs along with their frame number, imaging time and interval after the initial pressure transient (PT 1) generated by firing Impactor 3 alone.

Table 7. High-Speed Video Imaging of Impsctor 3 Fired Alone; D-204-1-4 ID No. 5; 4500 frames/sec.			
Figure, Frame Nos.	**Time (s)**	**Interval (ms)**	**Remarks**
2a, 346	**0.076667**	**-0.222**	**No action yet**
347	0.076889	0.000	First sign of cavitation bubbles. PT 1 appears on the pressure-time trace.
2b, 348	**0.077111**	**0.222**	**Full cavitation throughout the water.**
2c, 349	**0.077333**	**0.444**	**Vertical column of cavitation bubbles plus a disk of cavitation bubbles**
			on the impactor.
350	0.077556	0.667	Column of bubbles diminishes. Disk of bubbles remains strong.
351	0.077778	0.889	Column of bubbles diminishes. Disk of bubbles remains strong.
352	0.078000	1.111	Column of bubbles diminishes. Disk of bubbles remains strong.
353	0.078222	1.333	Column of bubbles very faint. Disk of bubbles remains strong.
2d, 355	**0.078667**	**1.778**	**Column of bubbles has disappeared. Disk of bubbles remains strong.**
358	0.079333	2.444	Start of centered cavitation bubble. Diameter of disk of bubbles is decreasing.
			PT 2 appears on the pressure-time trace between Frames 358 and 359.
2e, 359	**0.079556**	**2.667**	**The centered cavitation bubble continues to grow. The diameter of**
			the disk of bubbles is decreasing.
360	0.079778	2.889	Centered cavitation bubble grows. Diameter of disk of bubbles is decreasing.
361	0.080000	3.111	Centered cavitation bubble grows. Diameter of disk of bubbles is decreasing.
2f, 362	**0.080222**	**3.333**	**Image of centered cavitation bubble remains strong. Diameter of disk**
			of bubbles on the impactor still seems to be decreasing; it disappears
			3 frames later. Centered cavitation bubble disappears 10 frames later,
			in Frame 372.

In Figure 7, we have reproduced several images from the high-speed video record of experiment D-204-1-4. (Note: The photographs chosen for Figure 7 are indicated in Table 7 by bold type.) The captions above the two peaks in Figure 6, PT 1 and PT 2, correlate the images in Figure 7 with two significant events that occurred in the water at the times these transients were generated:

- Many tiny cavitation bubbles were produced throughout the volume of the water when the initial pressure transient, PT 1, was generated (Frame 348).

- There was a diaphragm-type flexure of the upper plate of the impactor accompanied by a single large cavitation bubble when the second pressure transient, PT 2, was generated (Frames 358 and 359).

Steam Explosion of a Drop of Molten Ferrosilicon (D-199-1-4)

The experimental parameters associated with experiment D-199-1 are summarized in Tables 3a and b. In this experiment, we released a 1.23 g drop of molten FeSi75 into a pool of water at room temperature. The drop was allowed to fall 255 mm in water before it activated the photodetector, which then fires the mechanical impactor and starts the high speed video camera. Due to delays in the electrical circuit, the impactor is fired a little bit later, allowing the drop to fall to about 280 mm before it experiences the shock wave from the impactor. The shock wave will induce a collapse of the boiling film surrounding the drop and consequently initiates the steam explosion. The resulting pressure-time trace from this interaction is shown in Figure 8.

As in the previous section, we have again photographed the video monitor to record a number of selected high-speed video images from this experiment for comparison with the pressure–time trace shown Figure 8. In Table 8, we have described these photographs along with their frame number, imaging time and interval after the initial triggering transient generated by the impactor.

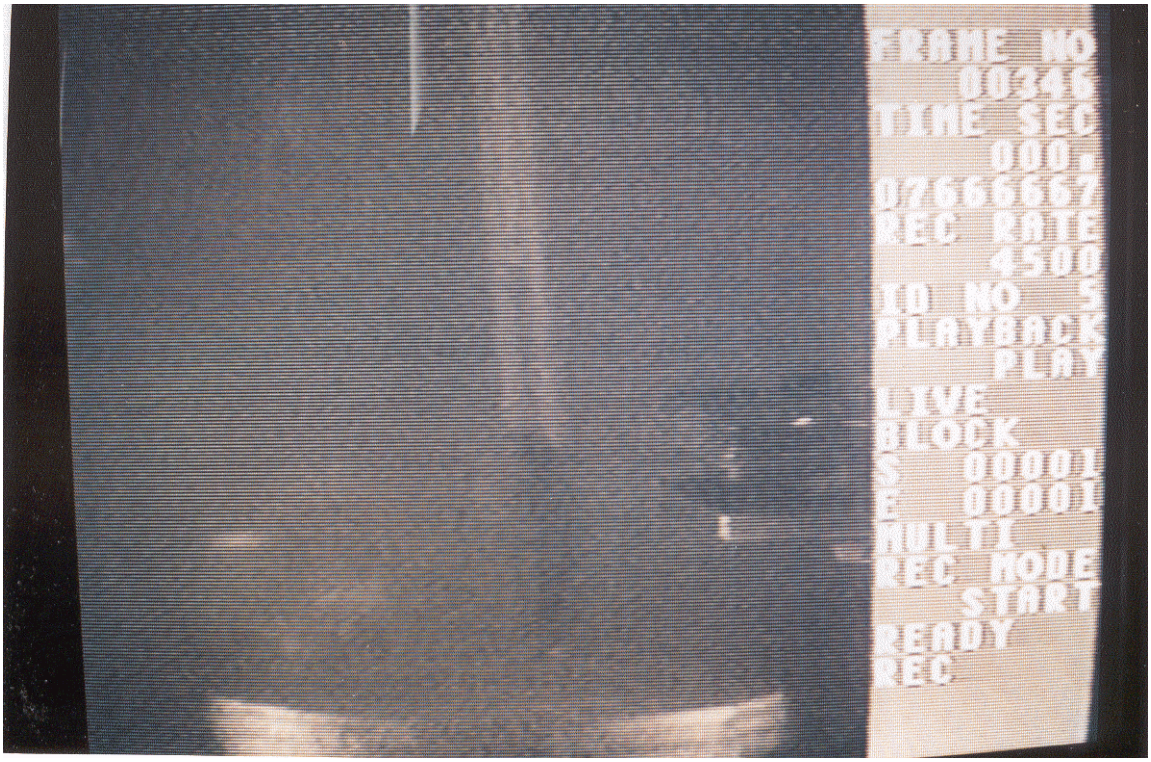

Figure 7a. High-speed video images of the firing of Impactor 3 alone (D-204-1-4). Frame 346, 0.222 ms before the impactor fired. No action yet. The pressure-time trace generated during this experiment is shown in Figure 6.

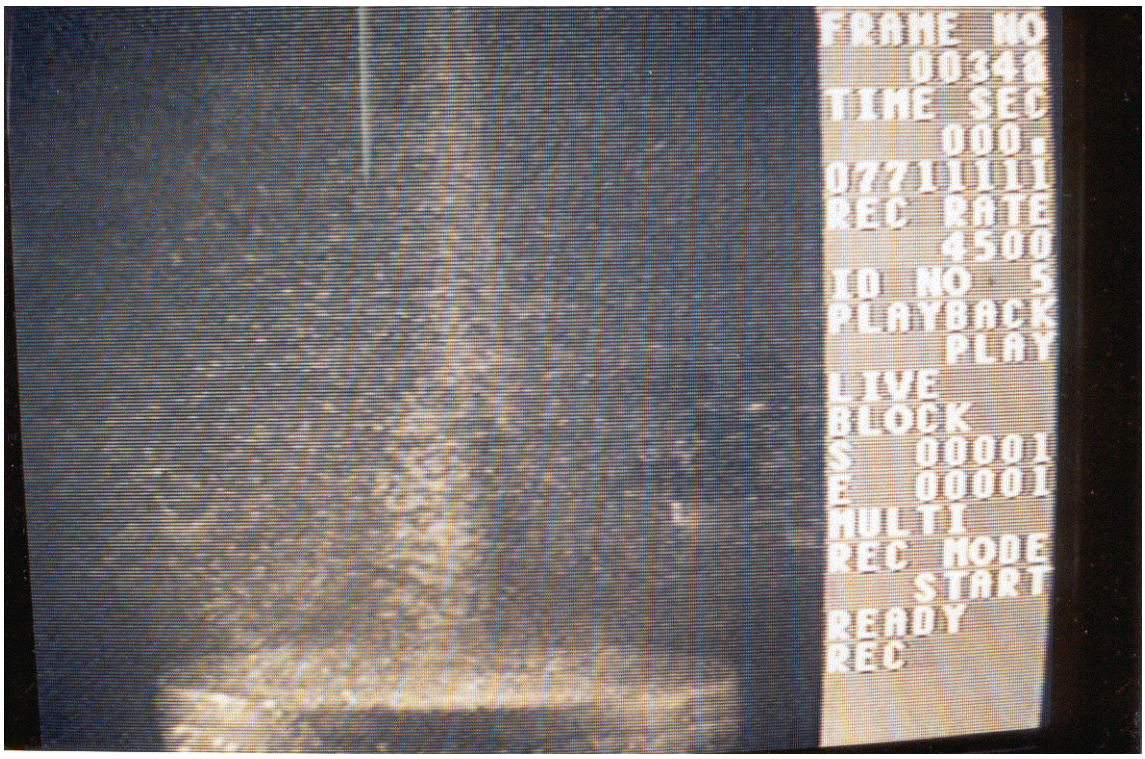

Figure 7b. High-speed video images of the firing of Impactor 3 alone (D-204-1-4). Frame 348, 0.222 ms after the impactor fired. There is full cavitation throughout the water. The pressure-time trace generated during this experiment is shown in Figure 6.

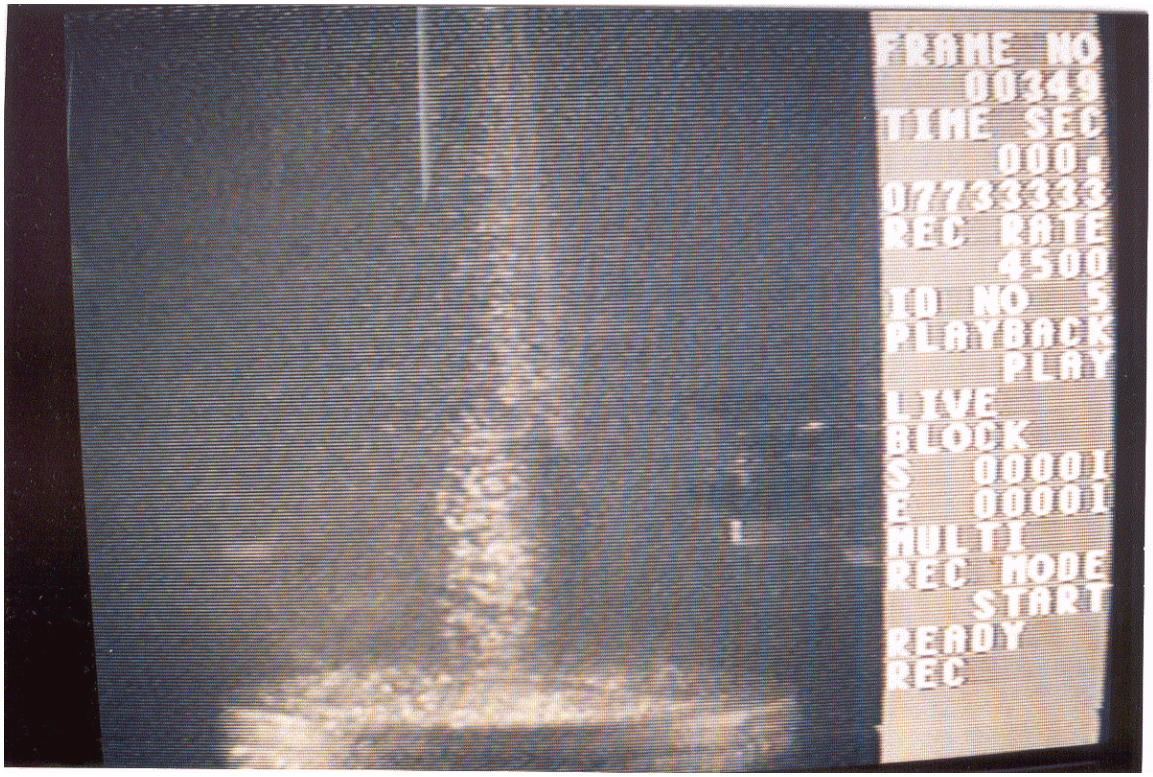

Figure 7c. High-speed video images of the firing of Impactor 3 alone (D-204-1-4). Frame 349, 0.444 ms after the impactor fired. There is a vertical column of cavitation bubbles in the water plus a disk of cavitation bubbles on the impactor's surface. The pressure-time trace generated during this experiment is shown in Figure 6.

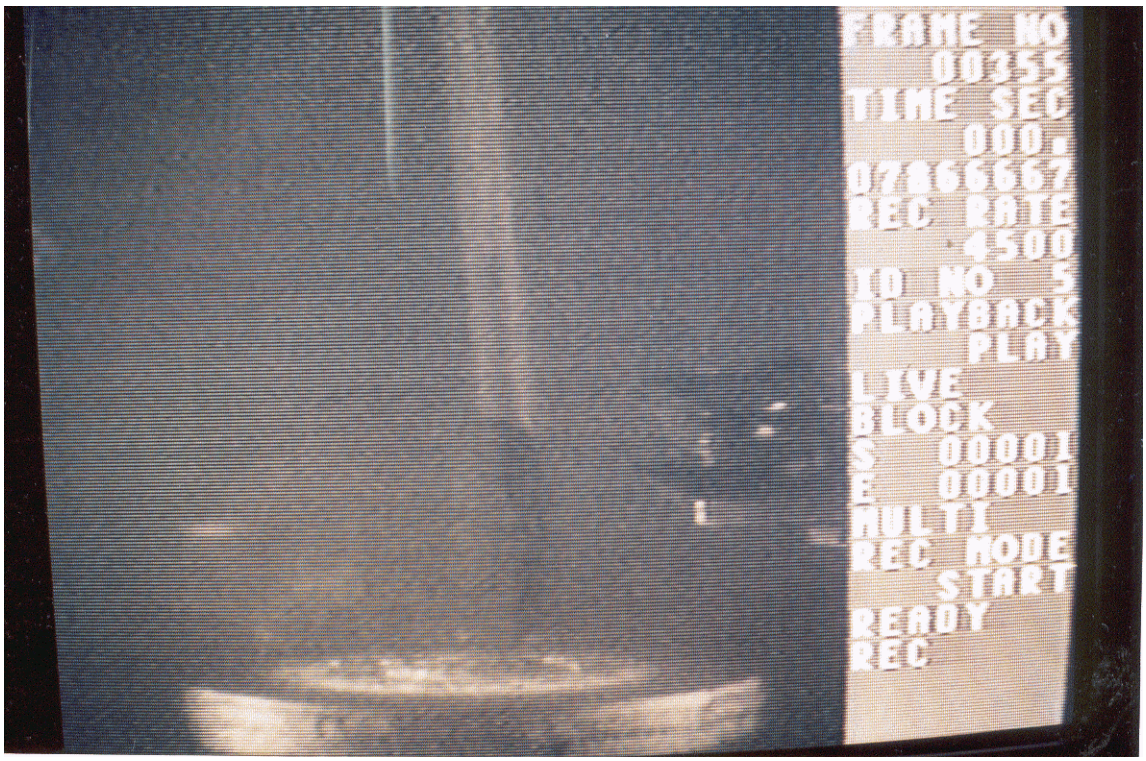

Figure 7d. High-speed video images of the firing of Impactor 3 alone (D-204-1-4). Frame 355, 1.778ms after the impactor fired. The vertical column of cavitation bubbles has disappeared. The image of the disk of bubbles remains strong. The pressure-time trace generated during this experiment is shown in Figure 6.

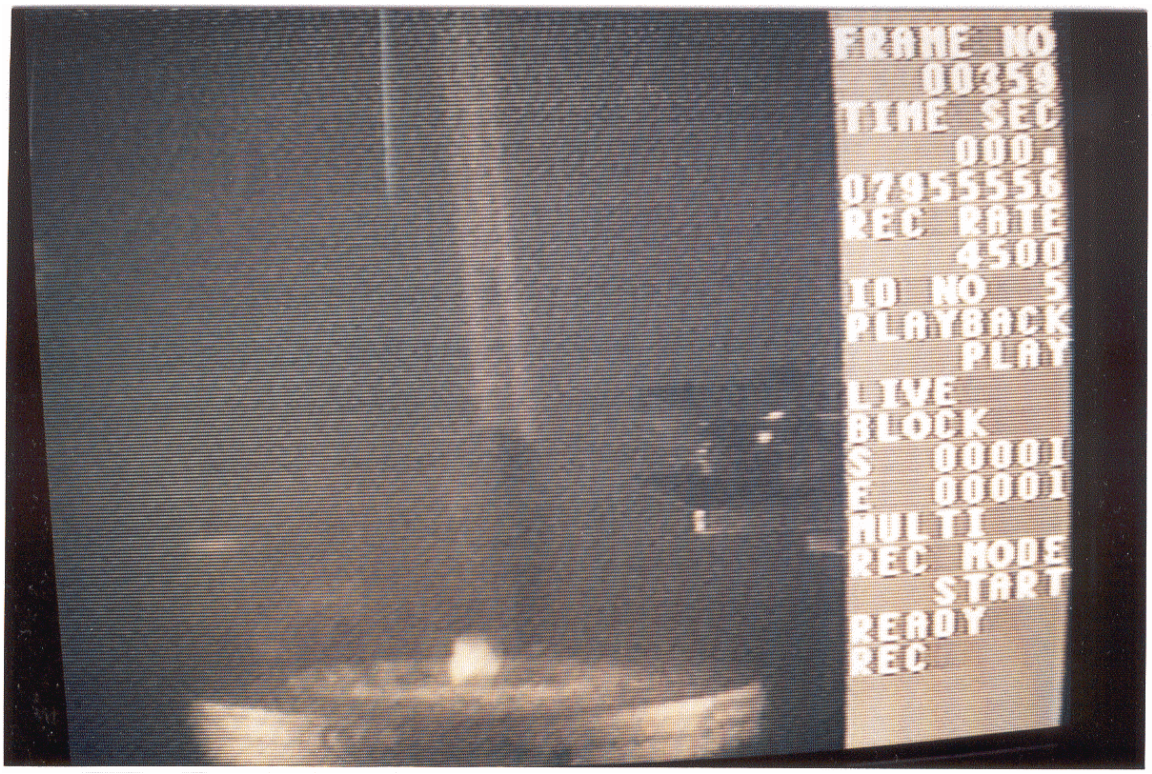

Figure 7e. High-speed video images of the firing of Impactor 3 alone (D-204-1-4). Frame 359, 2.667 ms after the impactor fired. The centered cavitation bubble continues to grow. The diameter of the disk of bubbles is decreasing. The pressure-time trace generated during this experiment is shown in Figure 6.

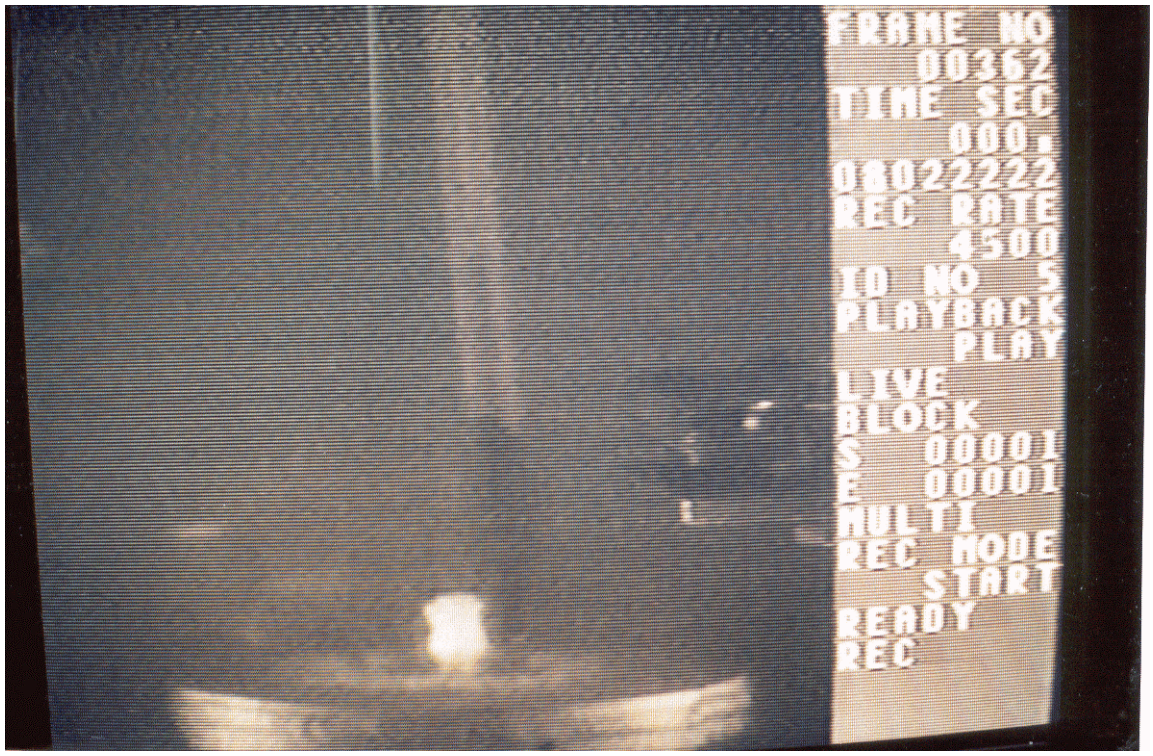

Figure 7f. High-speed video images of the firing of Impactor 3 alone (D-204-1-4). Frame 362, 3.333 ms after the impactor fired. Image of centered cavitation bubble remains strong. Diameter of disk of bubbles on the impactor is decreasing. The pressure-time trace generated during this experiment is shown in Figure 6.

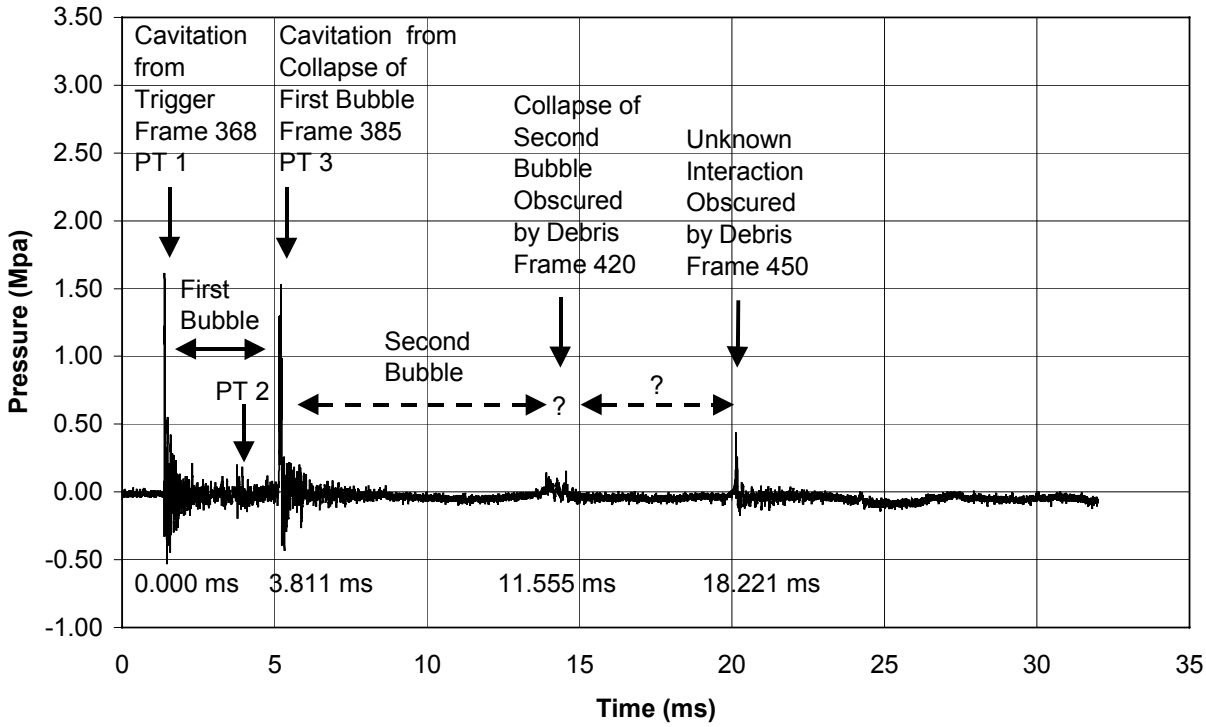

Figure 8. Pressure-time trace generated by the explosion of a drop of molten ferrosilicon with high-speed video imaging. (D-199-1-4).

In Figure 9, we have reproduced several images from the high-speed video record of experiment D-199-1-4. (Note: The photographs chosen for Figure 9 are indicated in Table 8 by bold type.) We shall now attempt to correlate the images listed in Table 8 and shown in Figure 9 with actions that occurred in the water at the times indicated.

The first peak in Figure 8 (PT 1) is the typical pressure peak associated with the firing of the mechanical impactor, as described earlier. We cannot observe the shock wave directly on the high-speed video images, but formation of cavitation bubbles in the water indirectly indicates that a shock wave has just passed. We were also able to observe a change in the appearance of the impactor surface, indicating that the surface was hit from below of the pressure-driven slug. This happened one frame (0.222 ms) before the frame of the cavitation bubbles (Frame 368 in Figure 9b). In the next frame, the cavitation bubbles have disappeared, and the luminosity from the molten drop increases. Following is a further increase in the size of the image, believed to be the growth of a steam bubble, and enhanced illumination. The growth continues for another 1.33 ms, before it stops at the first maximum (Frame 379 in Figure 9c). The size of the luminous steam-melt mixture then remains constant for 0.5 ms. Although the actual physical dimensions of the maximum bubble cannot be determined accurately from the video images due to overexposure, we have compared it with the image of the initial drop (also overexposed). The diameter of the first maximum image appears to be about three times larger than the diameter of the image of the luminous drop before the trigger was applied (Frame 366 in Figure 9a).

The bubble then collapses for approximately 4 frames (0.9 ms) before the formation of cavitation bubbles is seen again (Frame 385 in Figure 9d), and this frame corresponds time-wise to the second pressure peak from the steam explosion (PT 3) shown in Figure 8. (Peak PT 2 is the secondary pulse generated by the impactor; see Figures 2 and 6.) It is evident that peak PT 3 results from the collapse of the steam bubble and the subsequent water impact at its center. This is also confirmed by the fact that the drop's image starts to grow in the next frame, together with the formation of more cavitation bubbles (Frame 385, Figure 9d). The cavitation bubbles are also seen on the next frame (Frame 386, Figure 9e); thus they appear on three frames total. A question that arises is why these cavitation bubbles can be seen for such a long time (~0.6

Table 8. High-Speed Video Imaging of the Explosion of a Drop of Molten Ferrosilicon, D-199-1-4			
ID No. 2; 4500 Frames/Second			
Figure, Frame Nos.	Time (s)	Interval (ms)	Remarks
4a, 366	**0.081111**	**-0.444**	**Only the image of the luminous drop is seen. No action yet.**
367	0.081333	-0.222	Slight cavitation from impactor begins.
4b, 368	**0.081556**	**0.000**	**Cavitation from impactor is pronounced. Explosion is triggered.**
369	0.081778	0.222	Image of luminous drop begins to grow.
370	0.082000	0.444	Image of luminous drop continues to grow.
371	0.082222	0.667	Image of luminous drop continues to grow.
372	0.082444	0.889	Image of luminous drop grows further. Cavitation bubble at impactor begins.
373	0.082667	1.111	Image of luminous drop grows further. Cavitation bubble at impactor grows.
374	0.082889	1.333	Image of luminous drop grows further. Cavitation bubble at impactor grows.
375	0.083111	1.555	Image of luminous drop grows further. Cavitation bubble at impactor grows.
376	0.083333	1.778	Image of luminous drop grows further. Cavitation bubble at impactor grows.
377	0.083556	2.000	Image of luminous drop grows further. Cavitation bubble at impactor grows.
378	0.083778	2.222	Image of luminous drop grows further. Cavitation bubble at impactor grows.
4c, 379	**0.084000**	**2.444**	**Image of the luminous drop at the 1st maximum. Cavitation bubble at**
			the impactor is very distinct.
380	0.084222	2.666	Image of luminous drop decreasess. Cavitation bubble at impactor distinct.
381	0.084444	2.889	Image of luminous drop decreasess. Cavitation bubble at impactor distinct.
382	0.084667	3.111	Image of luminous drop decreasess. Cavitation bubble at impactor distinct.
383	0.084889	3.333	Image of luminous drop decreasess. Cavitation bubble at impactor distinct.
384	0.085111	3.555	Image of luminous drop decreasess. Cavitation bubble at impactor distinct.
4d, 385	**0.085333**	**3.777**	**Cavitation bubbles form from collapse of 1st bubble. Cavitation bubble**
			at impactor is still distinct.
4e, 386	**0.085556**	**4.000**	**Cavitation bubbles from collapse of 1st bubble grow larger. Cavitation**
			bubble at impactor is still distinct.
387	0.085778	4.222	Cavitation bubbles disappear. Image of luminous drop begins to grow again.
			Cavitation bubble at impactor is still distinct.
389	0.086222	4.666	Image of luminous drop grows further. Cavitation bubble at impactor distinct.
392	0.086889	5.333	Image of luminous drop grows further. Cavitation bubble at impactor distinct.
4f, 397	**0.088000**	**6.444**	**Image of the uminous drop is at 2nd maximum; it swallows the**
			cavitation bubble at the impactor.
401	0.088880	7.324	Image of luminous drop decreases.
410	0.090888	9.332	Image of luminous drop decreases.
411	0.091111	9.555	Image of luminous drop decreases.
4g, 420	**0.093111**	**11.555**	**Image of luminous drop breaks up. Bubble is obscured by debris.**
430	0.095333	13.777	Image of luminous drop breaks up. Bubble is obscured by debris.
440	0.097555	15.999	Image of luminous drop breaks up. Bubble is obscured by debris.
4h, 450	**0.099777**	**18.221**	**Luminous drop is very broken up. Bubble is obscured by debris.**
460	0.102000	20.444	Luminous drop is very broken up. Bubble is obscured by debris.
470	0.104222	22.666	Luminous drop is very broken up. Bubble is obscured by debris.
480	0.106444	24.888	Luminous drop is very broken up. Bubble is obscured by debris.

ms). We note that the duration of the pressure peak is about 0.1 ms. The cavitation bubbles associated with the trigger pressure pulse lasted only one frame (Frame 368, Figure 9b), and the duration of the first peak was the usual 0.03 ms, a factor of three shorter than the explosion pulse. A possible explanation for the longer lifetime of the second set of cavitation bubbles is that the temperature of the water in which they form the second time may have increased significantly due to heat transferred from the melt particles during the initial fragmentation.

Following the collapse is another growth cycle, where the bubble reaches its largest diameter (Frame 397, Figure 9f). It is interesting to note that the bubble doubles its size compared to the first expansion bubble. The bubble grows for about 4 ms; then it starts to collapse again. Luminous particles are left behind the collapsing bubble, but they are somewhat pulled in against the center (approximately Frame 420, Figure 9g). The collapse lasts for another 4 ms, and during this time some of the luminosity of the drop is lost in

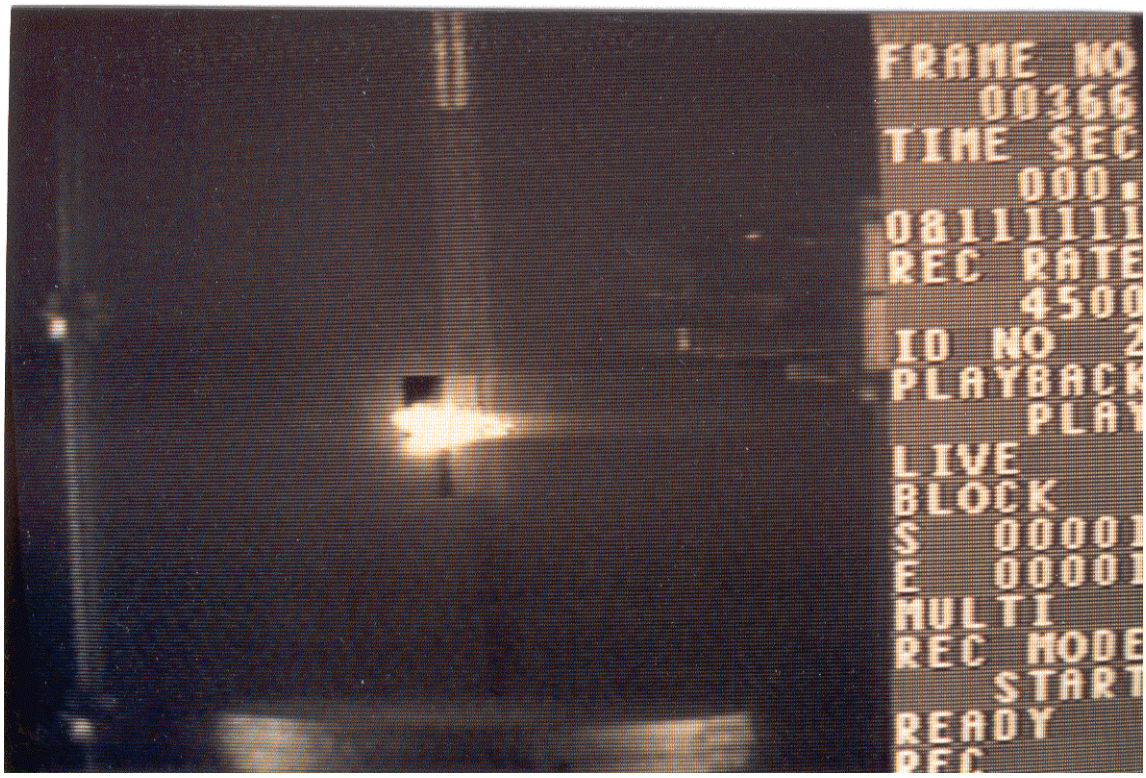

Figure 9a. High-speed video images of the explosion of a drop of molten ferrosilicon (FeSi75). (D-199-1-4). Frame 366, 0.444 ms before the trigger. Only the image of the luminous drop is seen. No action yet. The pressure-time trace generated during this experiment is shown in Figure 8.

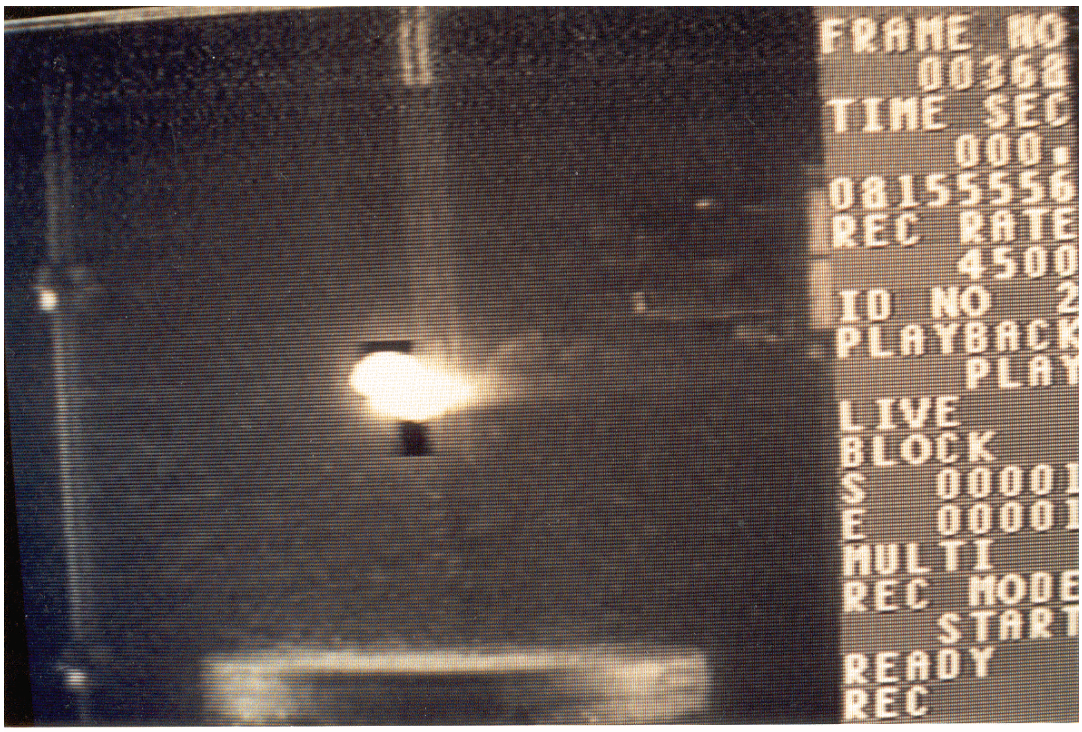

Figure 9b. High-speed video images of the explosion of a drop of molten ferrosilicon (FeSi75). (D-199-1-4). Frame 368 at triggering time. There are cavitation bubbles from the impactor pulse throughout the water. Explosion is triggered. The pressure-time trace generated during this experiment is shown in Figure 8.

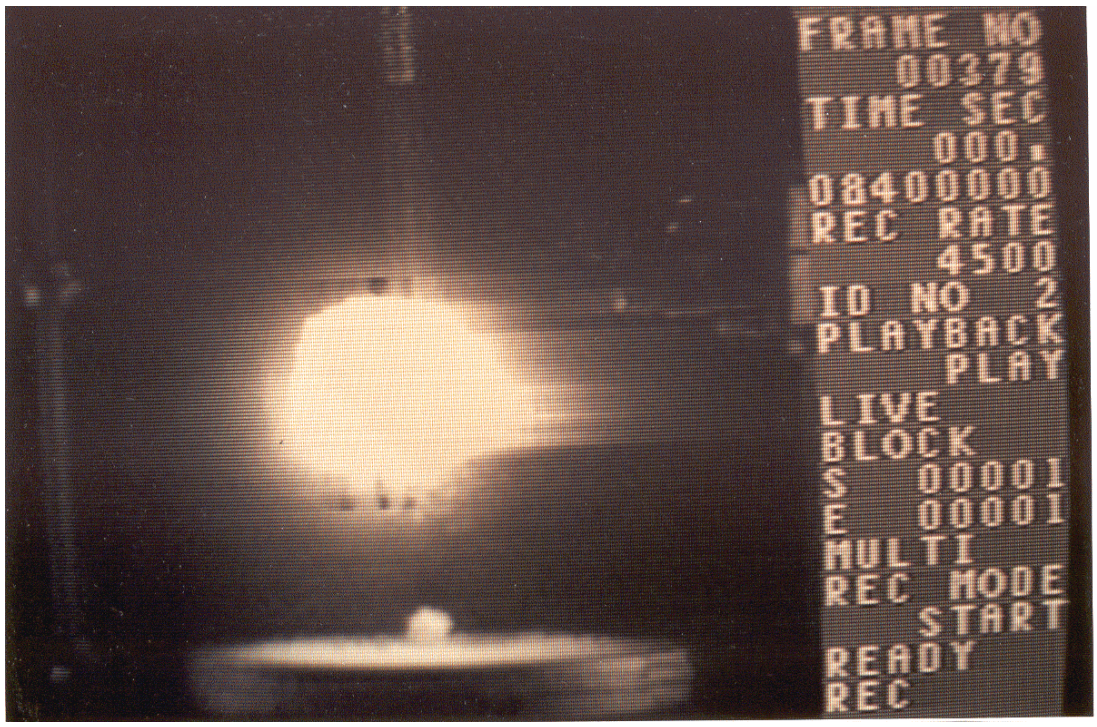

Figure 9c. High-speed video images of the explosion of a drop of molten ferrosilicon (FeSi75). (D-199-1-4). Frame 379 2.444 ms after the trigger. Image of the luminous material reaches the first maximum. Cavitation bubble at the impactor is very distinct. The pressure-time trace generated during this experiment is shown in Figure 8.

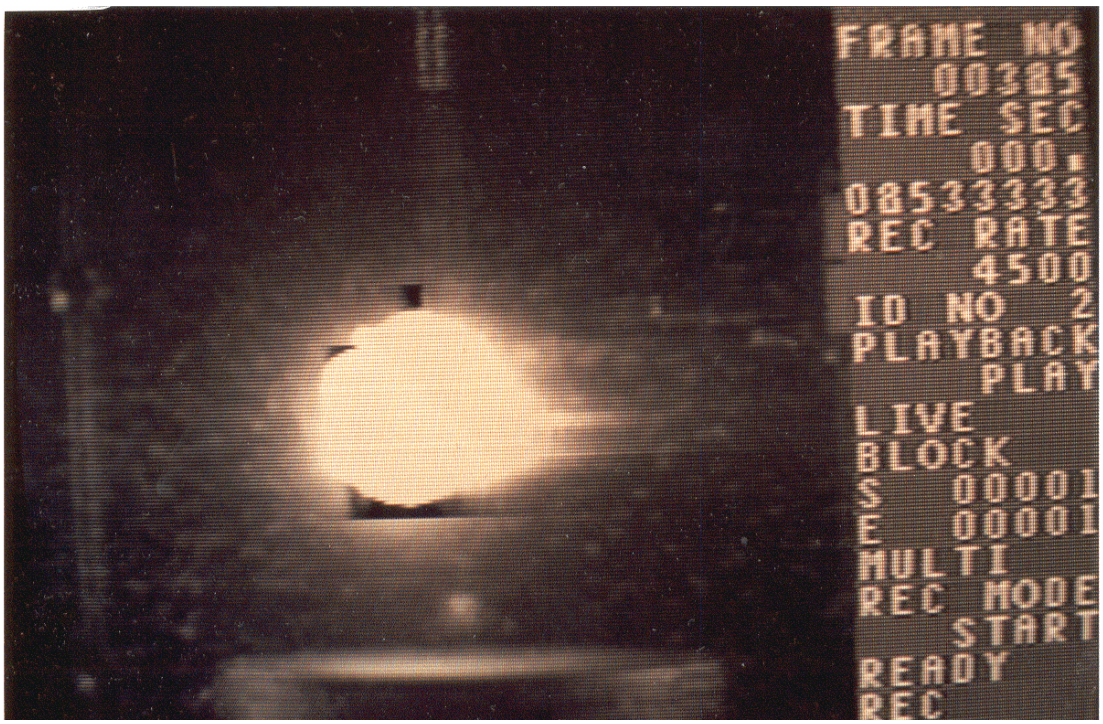

Figure 9d. High-speed video images of the explosion of a drop of molten ferrosilicon (FeSi75). (D-199-1-4). Frame 385 3.777 ms after the trigger. Cavitation bubbles form from the collapse of the first bubble. Cavitation bubble at the impactor is still distinct. The pressure-time trace generated during this experiment is shown in Figure 8.

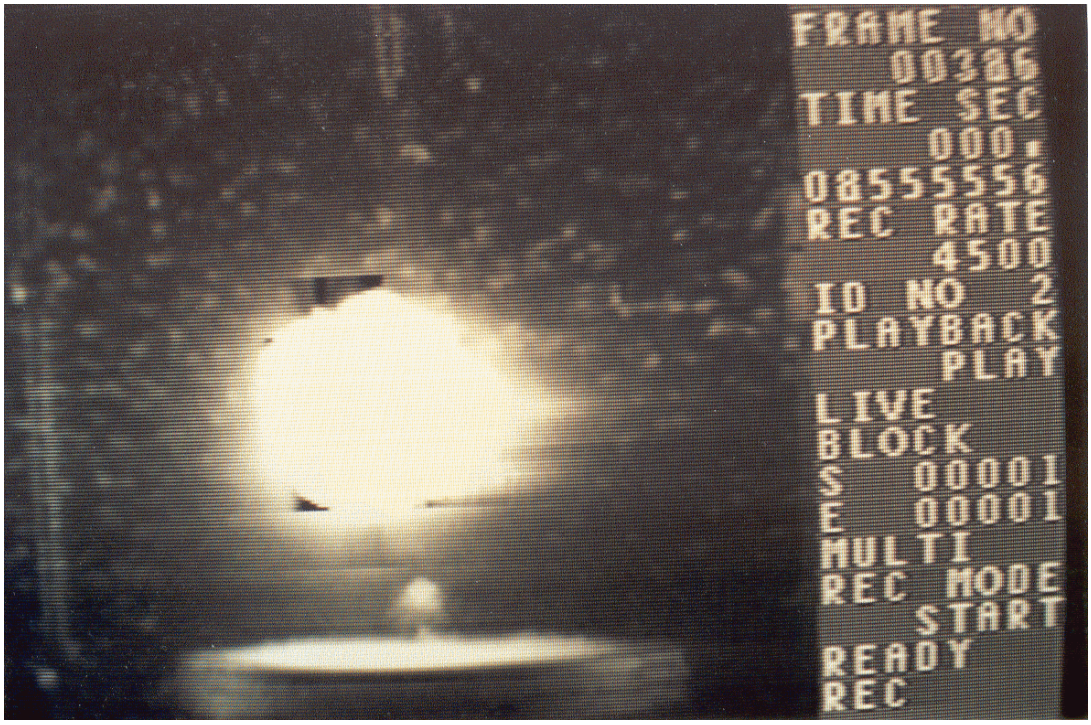

Figure 9e. High-speed video images of the explosion of a drop of molten ferrosilicon (FeSi75). (D-199-1-4). Frame 386 4.000 ms after the trigger. Cavitation bubbles from the collapse of first bubble grow larger. Cavitation bubble at impactor is still distinct. The pressure-time trace generated during this experiment is shown in Figure 8.

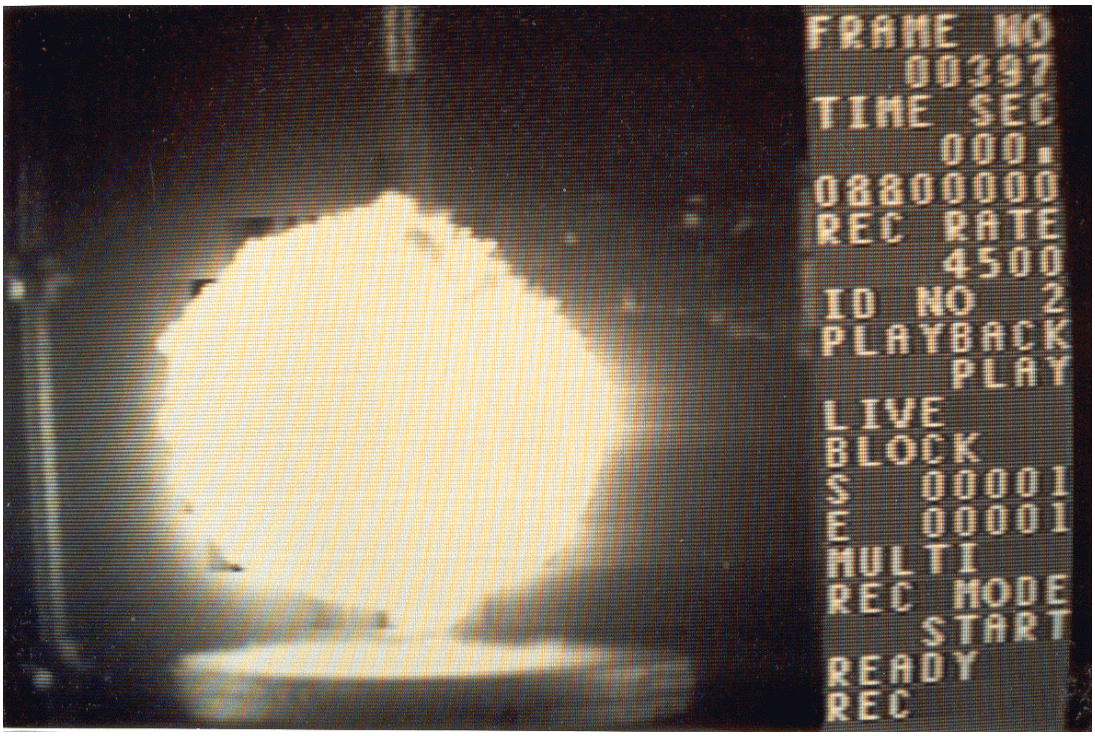

Figure 9f. High-speed video images of the explosion of a drop of molten ferrosilicon (FeSi75). (D-199-1-4). Frame 397 6.444 ms after the trigger. Image of the luminous material is at the second maximum; it swallows the cavitation bubble at the impactor. The pressure-time trace generated during this experiment is shown in Figure 8.

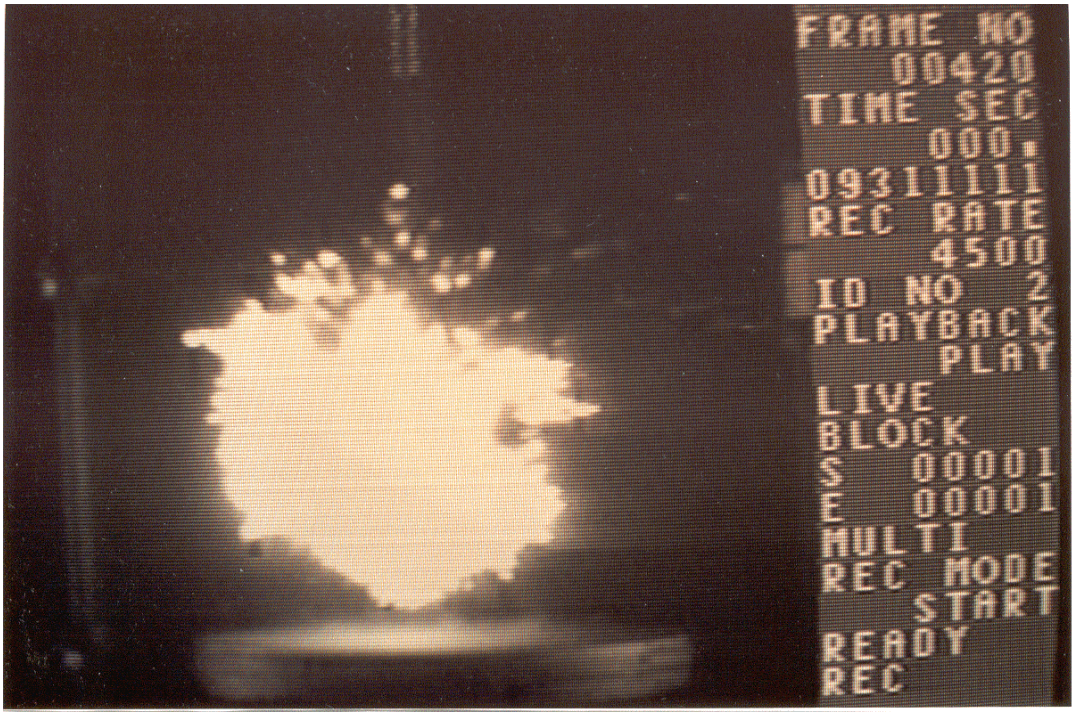

Figure 9g. High-speed video images of the explosion of a drop of molten ferrosilicon (FeSi75). (D-199-1-4). Frame 420 11.555 ms after the trigger. Image of the luminous drop breaks up. Bubble is obscured by debris. The pressure-time trace generated during this experiment is shown in Figure 8.

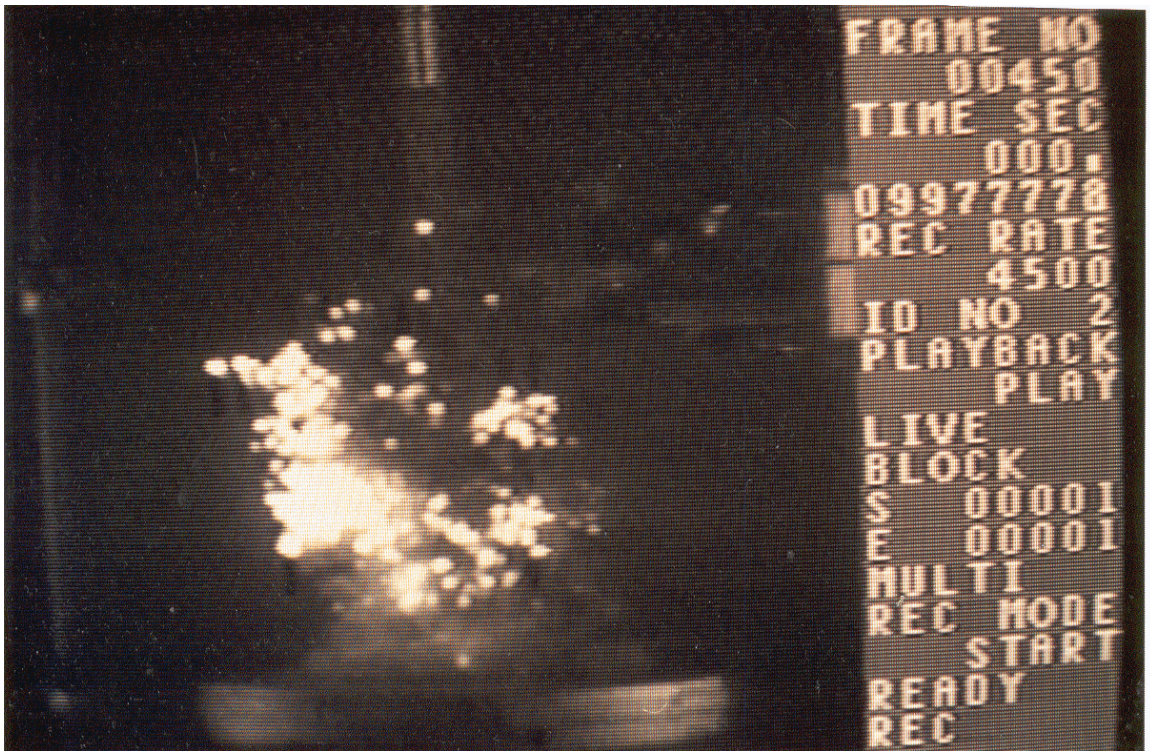

Figure 9h. High-speed video images of the explosion of a drop of molten ferrosilicon (FeSi75). (D-199-1-4). Frame 450 18.221ms after the trigger. Luminous material is very broken up. Bubble is obscured by debris. The pressure-time trace generated during this experiment is shown in Figure 8.

some areas. Then, when the bubble seems to be at its minimum again, a dark cloud of colloidal material is blown out from the lower parts of the bubble (between Frame 420, Figure 9g, and Frame 450, Figure 9h). This corresponds to the second of the small pressure peaks in Figure 8, after about 14 ms. It is interesting to note that even though we had a very large bubble, its collapse did not induce a strong pressure peak. Indeed, the first bubble, which was only half the size, created a much stronger pulse when collapsing. We can only speculate about the reasons, but if there is considerably more gaseous hydrogen in the second bubble, its collapse, when the water rushes inwards, will not produce an impact with the same strength as for a bubble that does not contain permanent gas. That is, it will merely slow down and bounce off the hydrogen-containing bubble, which will behave like a spring.

The cloud of dark material then starts to spread out, and grows for about 3.3 ms before it slows down and is relatively stable for a short time (two frames on the videotape). Then, apparently due to water jets accelerating inwards, the dark cloud is decreasing in size again. This is the start of another collapse, but this time it is quite different in appearance, as we now are able to see the particles. The dark cloud collapses until another dark cloud starts to form and expand accompanied by an increase in the emitted light. Again, the transition between collapse and expansion of a new bubble can be compared to the pressure trace in Figure 8 (Frame 450, Figure 9h), where this is exactly the position of the last peak pressure pulse, after 20 ms. The bubble grows for another 2 ms, then slows down and no further bubble cycles are seen. A mixture of dark colloidal material and several bright particles fill the area above the impactor.

We note that the very last pressure peak in Figure 8, related to the collapse of the second bubble of mostly dark colloidal material, is much stronger than its former bubble of the same kind. Again, we can only speculate that the gas composition of the bubble might have been different in the bubbles.

Steam Explosion of a Drop of Molten Silicon (D-202-1-4)

Experiment D-202-1-4 was a repetition of experiment D-199-1-4, except for the use of a drop of molten silicon instead of the drop of molten ferrosilicon. All other experimental parameters were essentially the same (see Tables 4a and b). Again, the event was recorded using the Ektapro high-speed video camera together with the pressure transducer. We obtained a very strong explosion that produced the pressure-time trace shown in Figure 10. The explosion ejected considerable water from the chamber and also dislodged our hydrogen measuring system from its mountings.

As in experiments D-204-1-4 and D-199-1-4, we again photographed the video monitor to record selected high-speed video images from this experiment for correlation with the pressure–time trace shown Figure 10. These images are listed in Table 9 and some of the photographs are reproduced in Figure 11.

In Frame 364, the video image (Figure 11a) shows the luminous drop as it falls through the water just before the interaction is triggered. One frame later, in Frame 365, a few tiny cavitation bubbles are seen in the water, while in the next, Frame 366, a large number of tiny cavitation bubbles is observed (Figure 11b), together with the movement of the impactor surface. We assume this activity coincides with the first large peak, PT 1, that results from the firing of the impactor and assign Frame 366 the starting time of 0.000 ms.

On the order of 0.2 ms after the passage of the pressure front, the image of the luminous drop starts to grow. We assume this to indicate the rapid onset of fragmentation and enhanced steam production. The mixture of molten silicon and steam expands and reaches a maximum in Frame 372 (Figure 11c) at 1.778 ms. We see that this corresponds to a quiet region in the pressure-time trace.

About 1 ms after the maximum, in Frame 377 (Figure 11d), cavitation bubbles are observed again at 2.888 ms, indicating the passage of another high-pressure front. This time corresponds exactly to the second large peak, PT 3, in Figure 10. (Note: The second pulse from the impactor at 2.6 ms, PT 2 (from the diaphragm-like flexure of its upper plate), can also be detected in Figure 10, but is almost hidden by the much larger pulse produced by the steam explosion.) Thus, we interpret the high pressure peak, PT 3, as the result of direct melt-water contact at the imagined center of the melt/gas mixture. This contact is assumed to arise

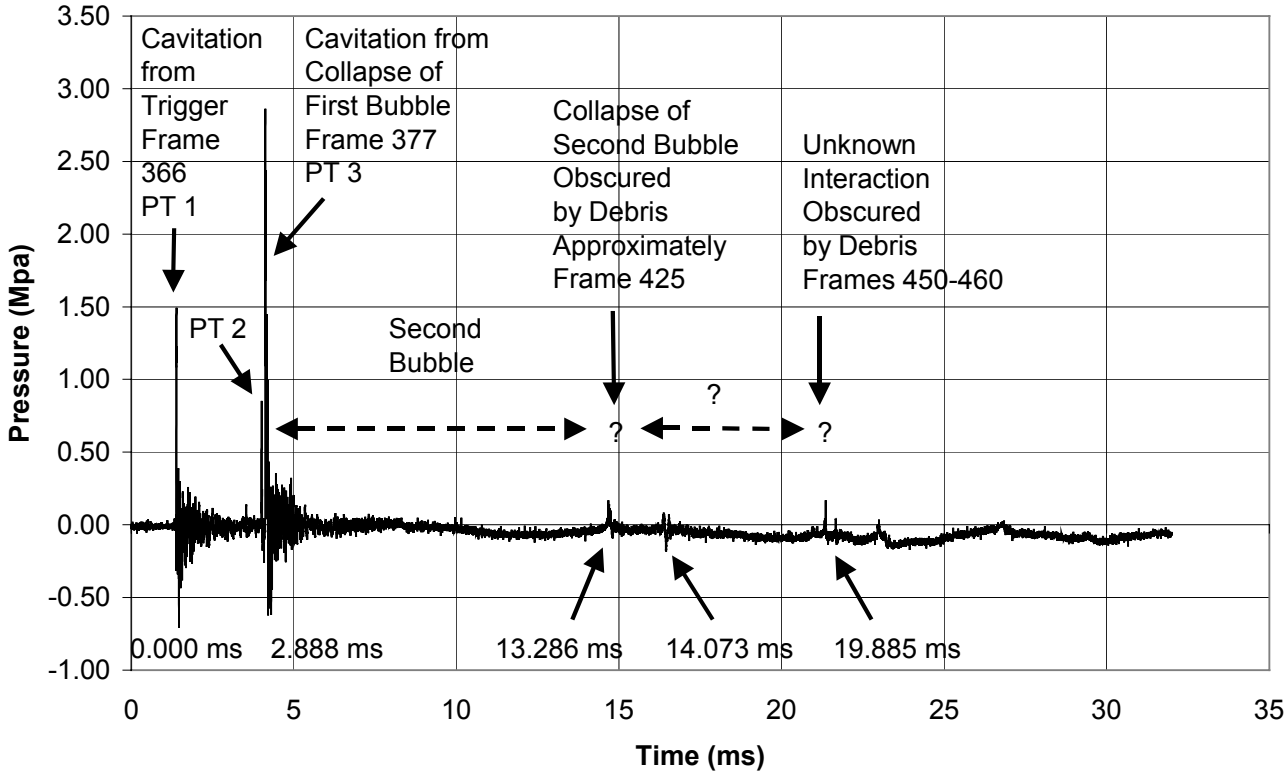

Figure 10. Pressure-time trace generated by the explosion of a drop of molten silicon with high-speed video imaging. (D-202-1-4).

from the collapse of the bubble, which may leave a region with lower pressure than the surrounding water. Note that more and larger cavitation bubbles were formed by the second pressure transient, PT 3 (Figures 11d and 11e) than by the triggering pulse, PT 1 (Figure 11b). This is consistent with the much higher peak pressure of PT 3 than of PT 1—almost twice as high—as shown in Figure 10.

The passage of a second pressure pulse strong enough to create cavitation bubbles induces further fragmentation of the melt, with more steam generation. At this stage, the hydrogen generation becomes important, as we will see later. A new bubble growth-collapse cycle starts, and this second bubble grows much larger than the first. To see this, compare the images in Frame 395 at 6.889 ms (Figure 11f) and Frame 372 at 1.778 ms (Figure 11c).

We would expect that the large second bubble, shown in Frame 395 (Figure 11f), would initiate a strong pressure peak upon collapsing. But this was not found to be the case. Examining the images, the estimated time for the impact is close to 13.3 ms, approximately at Frame 425 (Figure 11g). (These images are partially obscured by the breakup of the luminous material and the formation of a cloud of fine debris.) The pressure-time trace shows only two small peaks at approximately this time, however, not at all the magnitude of the first two peaks. No cavitation bubbles are seen either. A possible explanation involves the hydrogen generation mentioned earlier. As the melt is fragmented, silicon will react with water vapor to produce hydrogen gas, which does not condense under these conditions. Thus, the bubble will contain a mixture of both steam and hydrogen gas. Upon collapsing, the steam will condense, but the hydrogen will not. The entrapped gas will behave similar to when a spring is compressed by slowing down the advancing water surface considerably. Therefore, the impact of the water on the melt does not result in a large pressure peak where we had expected it. If the reaction times involved in the silicon-water reaction are large compared with typical fragmentation times, this would explain why we do not observe the same effect for the first bubble, where the water impact creates a very large pressure peak. In this case, the generation of hydrogen is still too small to have any effect. Also, the generation of hydrogen is strongly related to the surface area of the melt, which is several times larger during the growth of the second bubble.

Table 9. High-Speed Video Imaging of the Explosion of a Drop of Molten Silicon, D-202-1-4 ID No. 4; 4500 Frames/Second			
Figure, Frame Nos.	**Time (s)**	**Interval (ms)**	**Remarks**
6a, 364	**0.080667**	**-0.444**	**Only the image of the luminous drop is seen. No action yet.**
365	0.080889	-0.222	Slight cavitation from impactor begins.
6b, 366	**0.081111**	**0.000**	**Cavitation from impactor is pronounced. Explosion is triggered.**
367	0.081333	0.667	Cavitation bubbles diminish. Image of luminous drop begins to grow.
368	0.081555	0.889	Image of luminous drop continues to grow.
369	0.081778	1.111	Image of luminous drop continues to grow.
370	0.082000	1.333	Image of luminous drop continues to grow.
371	0.082222	1.555	Image of luminous drop grows further. Cavitation bubble at impactor begins.
6c, 372	**0.082444**	**1.778**	**Image of the luminous drop at the 1st maximum. Cavitation bubble at**
			the impactor is growing.
373	0.082666	2.000	Image of luminous drop decreasess. Cavitation bubble at impactor is growing.
374	0.082889	2.222	Image of luminous drop decreasess. Cavitation bubble at impactor is growing.
375	0.083111	2.444	Image of luminous drop decreasess. Cavitation bubble at impactor is growing.
376	0.083333	2.666	Image of luminous drop decreasess. Cavitation bubble at impactor is growing.
6d, 377	**0.083555**	**2.888**	**Cavitation bubbles from collapse of 1st bubble are pronounced.**
			Cavitation bubble at the impactor is still growing.
6e, 378	**0.083777**	**3.111**	**Cavitation bubbles from collapse of 1st lbubble grow larger. Cavitation**
			bubble at the impactor is still growing. Image of luminous drop
			begins to grow again.
379	0.084000	3.333	Cavitation bubbles from collapse of 1st lbubble decrease. Cavitation bubble at
			impactor is still growing. Image of luminous drop grows further.
380	0.084222	3.555	Image of luminous drop grows further. Cavitation bubble at impactor distinct.
			Cavitation bubbles from collapse of 1st lbubble disappear.
381	0.084444	3.777	Image of luminous drop grows further, swallows cavitation bubble at impactor.
382	0.084666	3.999	Image of luminous drop grows further.
385	0.085333	4.667	Image of luminous drop grows further.
388	0.086000	5.333	Image of luminous drop grows further.
389	0.086222	5.556	Image of luminous drop grows further.
390	0.086444	5.778	Image of luminous drop grows further.
393	0.087111	6.444	Image of luminous drop grows further.
6f, 395	**0.087556**	**6.889**	**Image of luminous drop is at 2nd maximum.**
405	0.089778	9.111	Image of luminous drop decreases.
415	0.092000	11.333	Image of luminous drop decreases.
6g, 425	**0.094222**	**13.556**	**Image of luminous drop breaks up. Bubble is obscured by**
			debris.
430	0.095333	14.667	Image of luminous drop breaks up. Bubble is obscured by debris.
440	0.097556	16.889	Image of luminous drop breaks up. Bubble is obscured by debris.
450	0.097778	17.111	Image of luminous drop breaks up. Bubble is obscured by debris.
460	0.102000	21.333	Luminous drop is very broken up. Bubble is obscured by debris.
470	0.104222	23.556	Luminous drop is very broken up. Bubble is obscured by debris.
480	0.106444	25.778	Luminous drop is very broken up. Bubble is obscured by debris.
6h, 490	**0.108667**	**28.000**	**Luminous drop is very broken up. Bubble is obscured by**
			debris.
500	0.110889	30.222	Luminous drop is very broken up. Bubble is obscured by debris.

After the second collapse and the small pressure transients shown in Figure 10 at 13-14 ms, we observe a possible third bubble-growth cycle. However, this time, the silicon has cooled down considerably; in fact, on the images a black cloud of particles is thrown downwards from the center of explosion. There may still be some steam generation, but this is small compared to the earlier bubble cycles. The pressure-time trace shows only minor activity, which again is somewhat difficult to explain by comparing to the high-speed video images. As the melt cools, small particles are seen everywhere, most of them dark, but a few sparkling particles can also be seen (Frame 490, Figure 11h). These particles persist for a long time, some

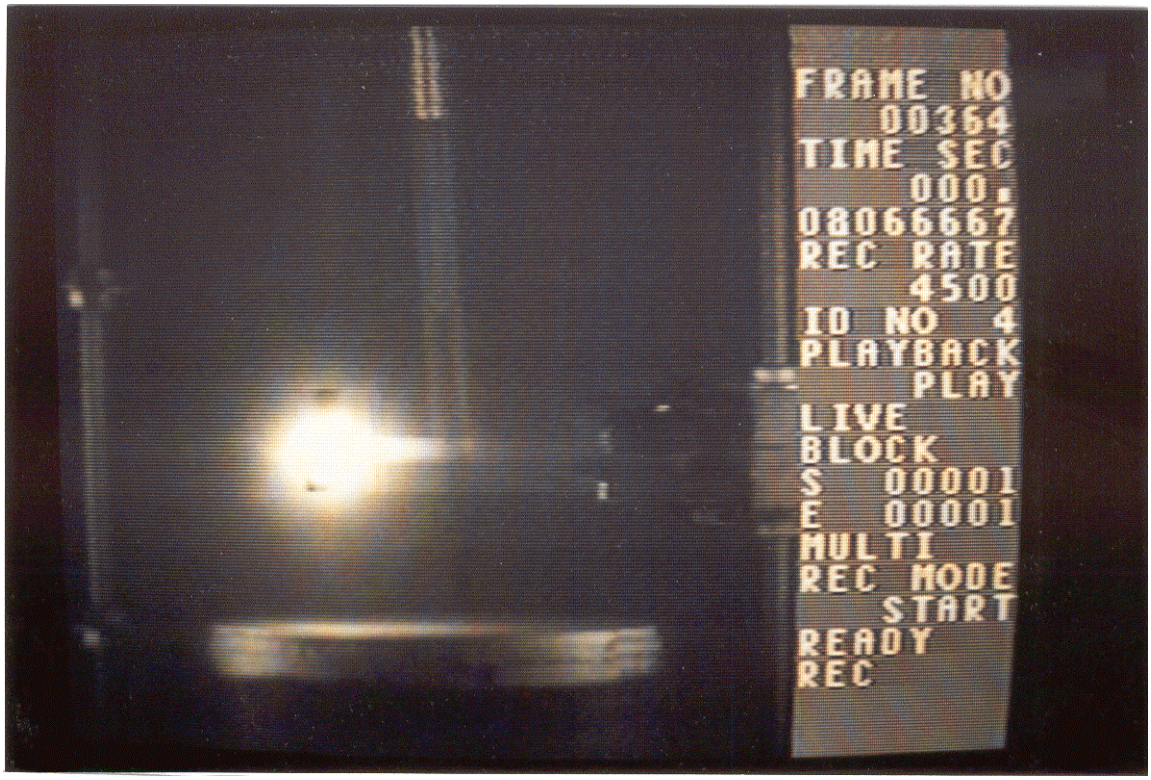

Figure 11a. High-speed video images of the explosion of a drop of molten silicon. (D-202-1-4). Frame 364 0.444 ms before the trigger. Only the image of the luminous drop is seen. No action yet. The pressure-time trace generated during this experiment is shown in Figure 10.

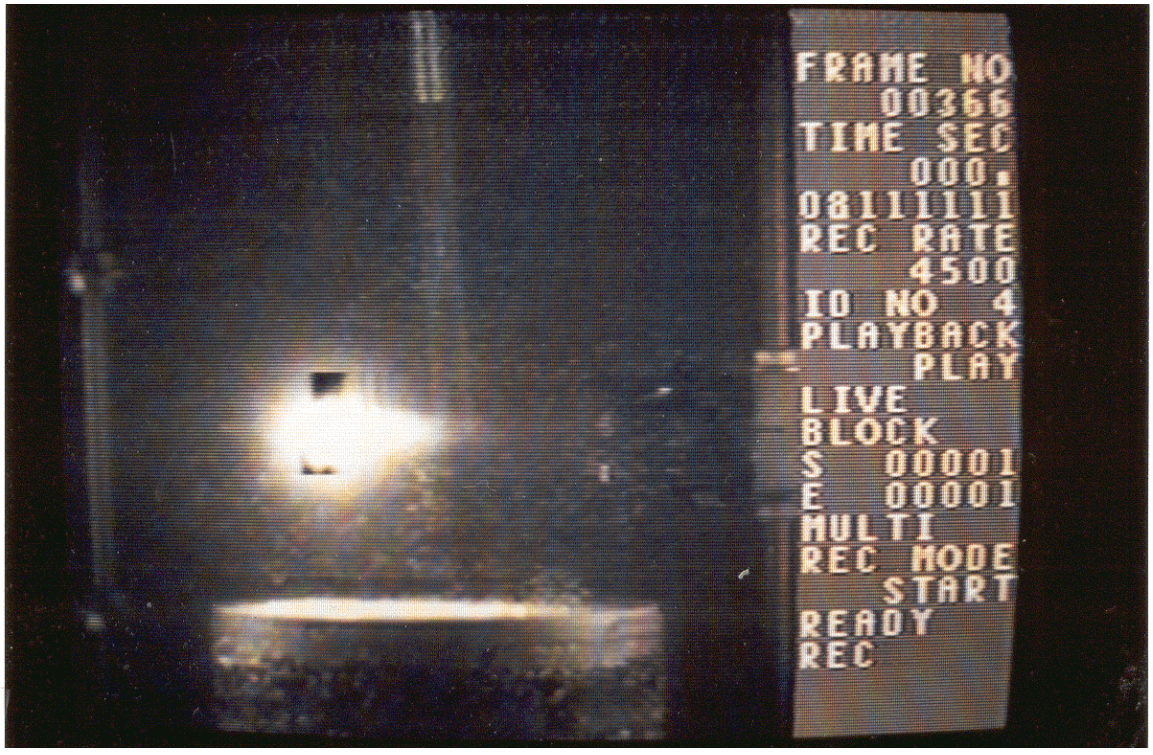

Figure 11b. High-speed video images of the explosion of a drop of molten silicon. (D-202-1-4). Frame 366 at triggering time. Cavitation bubbles from the impactor are pronounced. Explosion is triggered. The pressure-time trace generated during this experiment is shown in Figure 10.

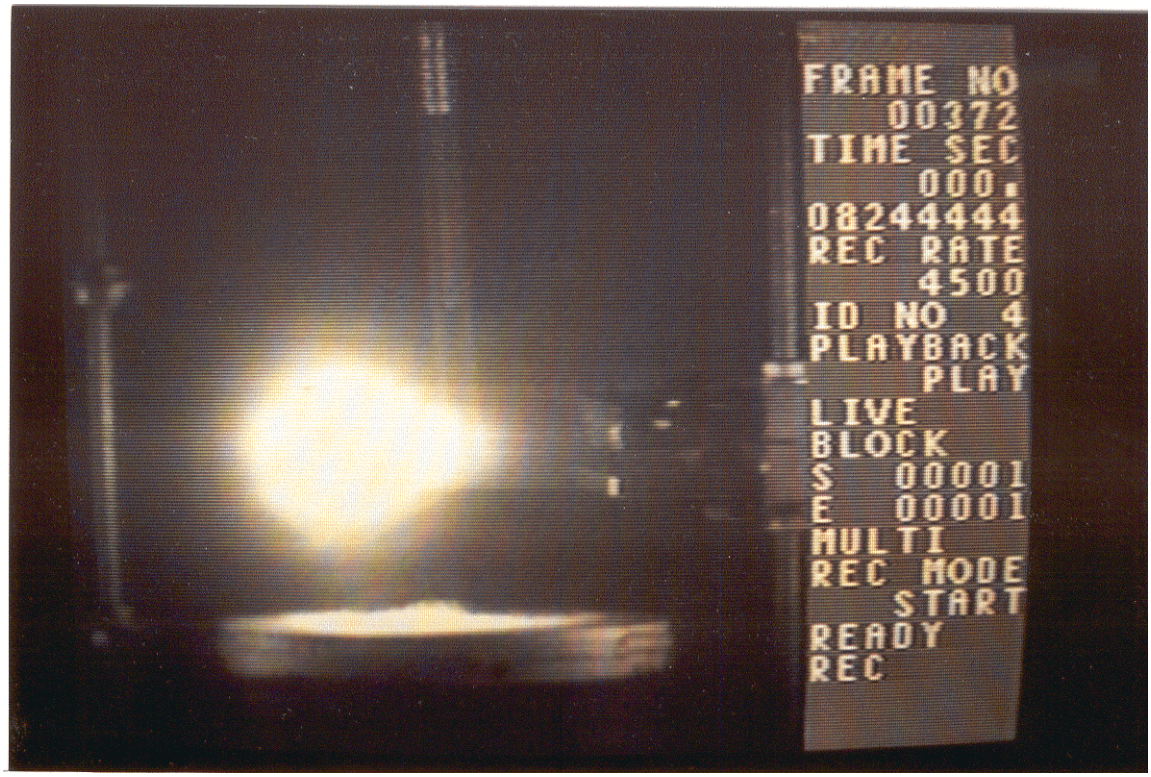

Figure 11c. High-speed video images of the explosion of a drop of molten silicon. (D-202-1-4). Frame 372 1.778 ms after the trigger. Image of the luminous material reaches the first maximum. Cavitation bubble at the impactor is growing. The pressure-time trace generated during this experiment is shown in Figure 10.

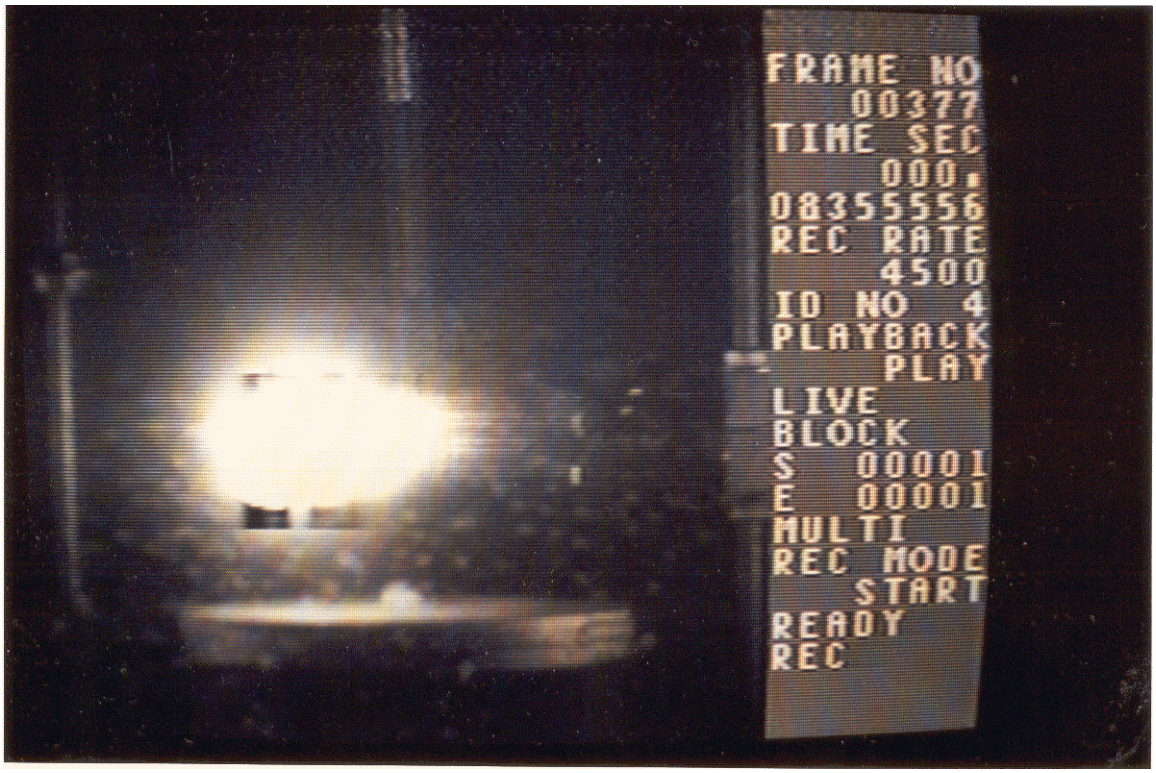

Figure 11d. High-speed video images of the explosion of a drop of molten silicon. (D-202-1-4). Frame 377 2.888 ms after the trigger. Cavitation bubbles form from the collapse of the first bubble. Cavitation bubble at the impactor is still growing. The pressure-time trace generated during this experiment is shown in Figure 10.

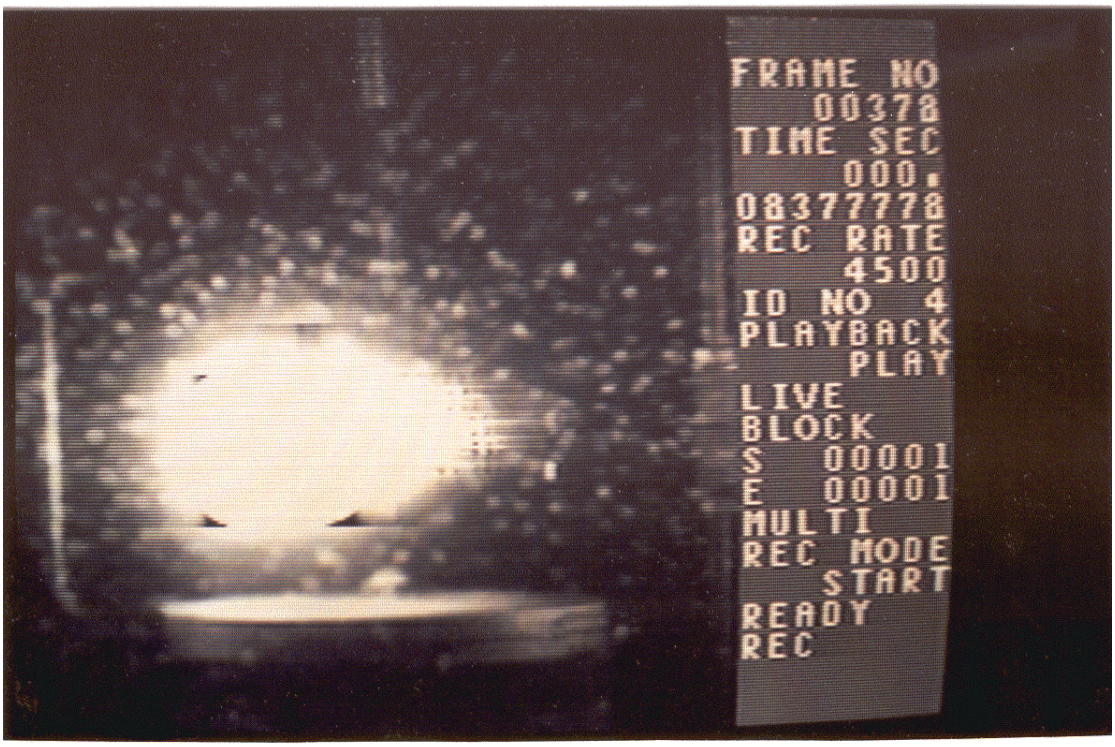

Figure 11e. High-speed video images of the explosion of a drop of molten silicon. (D-202-1-4). Frame 378 3.111 ms after the trigger. Cavitation bubbles from collapse of the first bubble grow larger. Cavitation bubble at the impactor is still growing. Image of luminous material begins to grow again. The pressure-time trace generated during this experiment is shown in Figure 10.

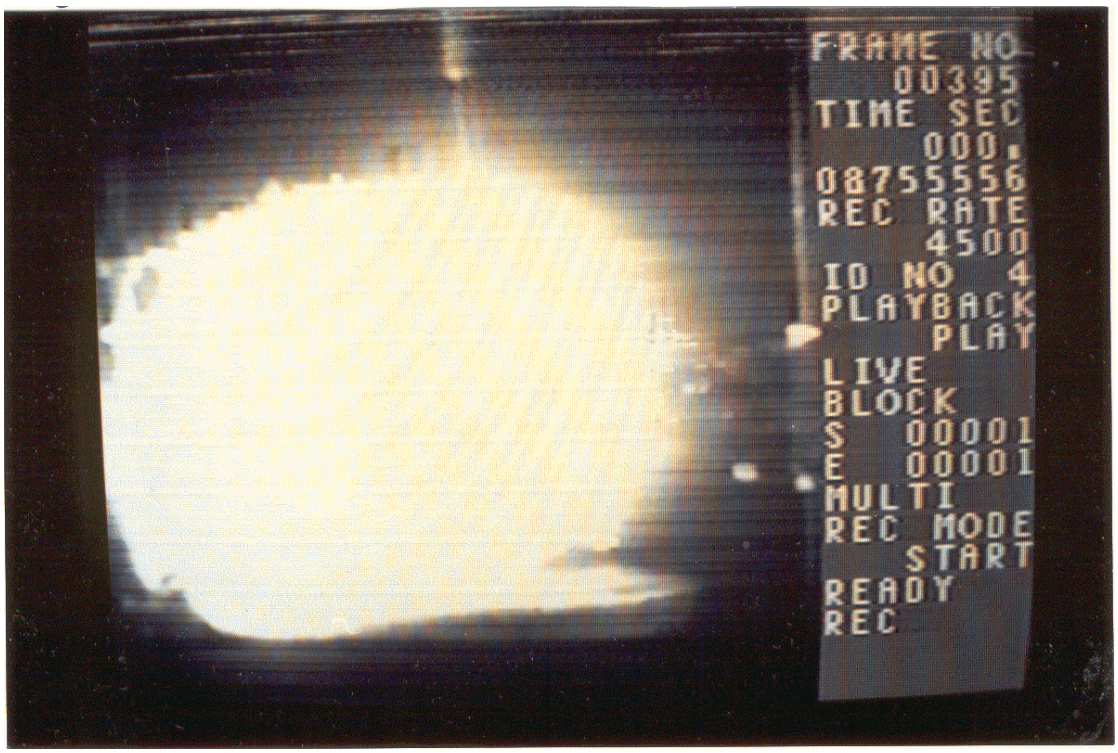

Figure 11f. High-speed video images of the explosion of a drop of molten silicon. (D-202-1-4). Frame 395 6.889 ms after the trigger. Image of luminous material reaches second maximum. The pressure-time trace generated during this experiment is shown in Figure 10.

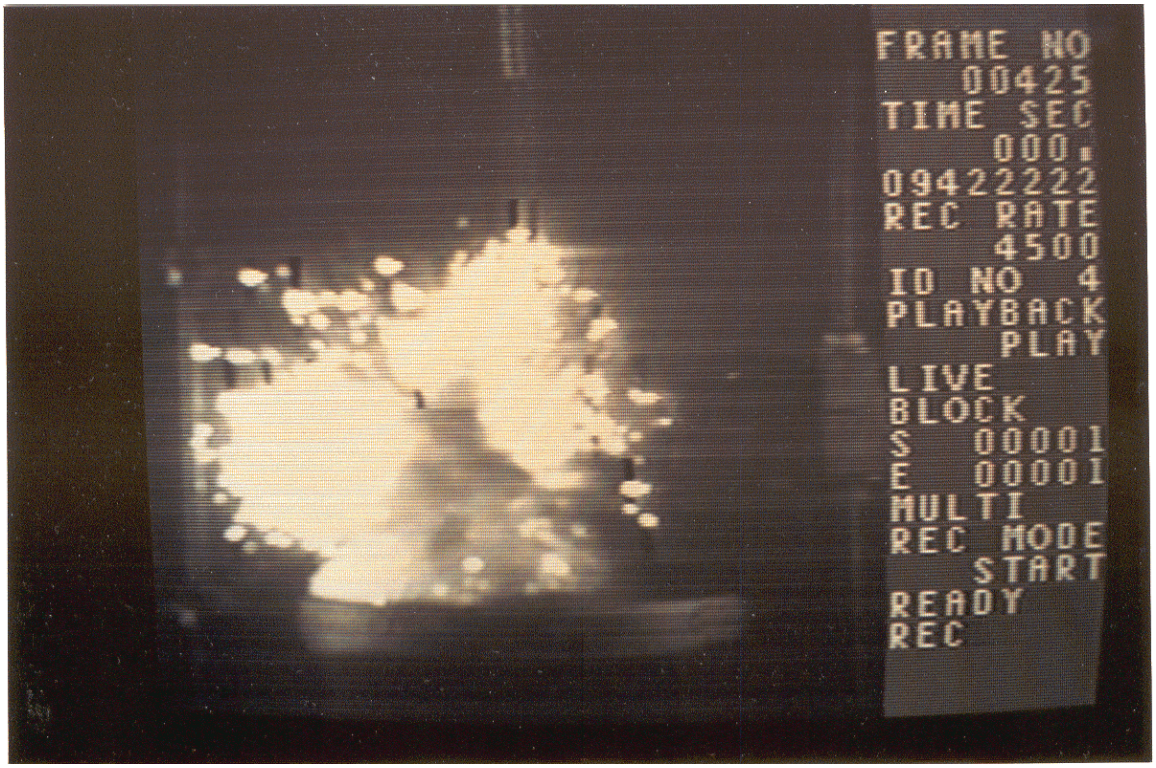

Figure 11g. High-speed video images of the explosion of a drop of molten silicon. (D-202-1-4). Frame 425 13,556 ms after the trigger. Image of luminous material breaks up. Bubble is obscured by debris. The pressure-time trace generated during this experiment is shown in Figure 10.

Figure 11h. High-speed video images of the explosion of a drop of molten silicon. (D-202-1-4). Frame 490 28.000 ms after the trigger. Luminous material is very broken up. Bubble is obscured by debris. The pressure-time trace generated during this experiment is shown in Figure 10.

as long as 150 ms after the triggering. Bubbles of hydrogen gas rise in the water, often carrying burning particles inside.

The duration of the main event is about 30 ms; after this, almost all of the melt has been converted into a black colloidal material, with a few sparkling particles that persist somewhat longer.

Drops of Molten Silicon Triggered at Various Depths

Nine experiments were performed with 9 mm-diameter drops of molten silicon that were exposed to peak triggering pulses in the range from 1.9 MPa to 4.9 MPa at depths in the water between 150 mm and 350 mm. These experiments are summarized in the order performed in Table 4a and sorted in order of depth of the impactor in Table 4b.

We found that:

- In 3 experiments where the peak triggering pressure applied to the drops was 3.4 MPa, one drop produced a strange, mild explosion (D-205-1), one drop produced a mild explosion with burning coarse particles (D-214-1), and the third, a very strong explosion that threw water (D-202-1).

- Strong explosions occurred when the peak triggering pressures were greater than 4 MPa (experiments D-223-1, D-207-1, D-209-1).

- In one experiment (D-197-1), the drop was exposed to a strong transient of 4.9 MPa but did not explode. Triggering was attempted here at the greatest depth, with the impactor at 400 mm.

- No explosion occurred in one experiment (D-191-2) when the peak pressure was 1.9 MPa.

- One experiment failed completely because of erratic drop motion (D-194-1).

These experiments indicate that explosions will occur when silicon drops are exposed (a) to a pressure transient greater than about 3.4 MPa when they are (b) at depths between about 150 mm and about 350 mm. These thresholds are in essential agreement with those presented in Table 3 of the Final Report for 1999 (Nelson et al., 2000).

Triggered Interactions of Drops of Molten Alloyed Silicon

During 2000, we looked further at how the steam explosions are affected by alloying the silicon rods from which the drops are prepared. This set of experiments essentially repeats similar work reported in the previous final report (Nelson et al., 2000), but with the addition of making pressure-time measurements during the triggered interactions.

Three experiments were performed, each with a drop prepared from one of the three rods taken from one of three batches of alloyed silicon used in the earlier work (Nelson et al., 2000). The weight percentages of the major elements alloyed with these rods are shown in Table 2 (see also Table A-1 in Appendix A).

The drops prepared from alloys B, C and D were exposed to triggering pulses between about 6 MPa and 11 MPa at a depth in the water of about 280 mm. These pulses were generated by Impactor 3 with its upper surface placed in the water at a constant depth of 300 mm and with the optical axis of the photodetector aimed horizontally 40 mm above it at a depth of 260 mm. These experiments are summarized in Table 5.

For comparison, we have included in this table one experiment—D-223-1–performed with a drop of nonalloyed silicon prepared from a rod taken from Batch A-5. (The parameters for experiment D-223-1

were also presented in Tables 4a and 4b.) The experimental parameters for this drop were nominally the same as for the three alloyed drops, except that the trigger pulse level was slightly lower–4.3 MPa.

The results obtained in 2000 (Table 5) were similar to those obtained in 1999 (Table 1C of Nelson et al., 2000): The drop prepared from Batch B (Al additive) (D-217-1) produced a very strong explosion that threw a lot of water and disabled our hydrogen collection apparatus (the strength of the explosion was similar to that of experiment D-202-1), while the drops prepared from Batches C (Ca additive) (D-219-1) and D (Al and Ca additives) (D-221-1) produced only mild interactions with coarse fragmentation of the melt. The drop of nonalloyed silicon (D-223-1) also produced a strong explosion, but not as strong as the explosion of the drop prepared from Batch B (Al additive) (D-217-1).

DISCUSSION

The Strong Pressure Transient PT 3

In the two experiments in which the explosions of drops of both molten silicon and ferrosilicon were imaged with the high-speed video camera, D-199-1-4 and D-202-1-4, we show conclusively that the dominant pressure transient generated in each explosion, PT 3, results from the collapse of the first and smaller bubble! We also show that although the second bubbles generated by both alloys may be much larger than the first, the pressure transient(s) they produce are much smaller than PT 3, although certainly not negligible. These results may be seen by comparing the pressure traces shown Figures 8 and 10 with their respective high-speed video images shown Figures 9 and 11.

In the previous sections, we have suggested that the smaller impacts generated by the larger bubbles are due to the chemical generation of hydrogen by the metal-water reaction concurrently with the thermal generation of steam during the explosions. Thus, when steam condenses in a collapsing bubble that also contains a permanent gas such as hydrogen, there is a cushioning effect that will reduce the pressure transient produced by the impact of the inrushing water.

We believe that much less hydrogen is generated during the growth of the first bubble than during the growth of the second because in the first event (a) there is less breakup of the melt, exposing a smaller surface area to the steam, and (b) the reaction time is shorter than in the second. Thus the cushioning by the hydrogen should be less during the collapse of the first bubble than of the second.

It should also be mentioned that if a large scale steam explosion of many silicon or ferrosilicon drops arrayed in water in a granulation tank (the "coarse premixture") somehow propagates by pressure transients generated by the individual drops, then the strong and only significant pressurization at PT 3 seems to be the most likely driver for the propagation.

Although the first and smaller bubble in both explosions has been identified in this report mainly with the high-speed video images recorded in reflected light in experiments D-199-1-4 and D-202-1-4, its formation has been detected often in the many explosions of both alloys that were recorded in a darkened room with time-exposed 35 mm photography. The smaller bubble appears on these images as the bright "golden" sphere at the center of a larger redder spherical image produced by the second bubble; both are produced by the luminosity of the highly fragmented melt particles as they move outward at the surface of the growing bubble. (Nelson and Duda (1982) have shown high-speed photographs of similar bubbles surrounded with glowing melt particles generated during the triggered steam explosion of drops of molten iron oxide.) In many of the experiments performed with both alloys during the years 1997 through 1999 (see Nelson et al., 1998, 1999a, 2000) and also during the year 2000 (see Tables 3a and b, 4 a and b and 5), these smaller bright, spherical images have appeared on the time-exposed images of the explosions; a particularly distinct example is shown in Figure 12 (D-217-1-4).

Finally, we note that the bubbles generated during explosions of melts that do not react chemically with the water will probably not experience the cushioning effect of the hydrogen during their collapse. Thus it is possible that the pressure transients generated during the collapse of the second and subsequent bubbles could be as large as or even larger than that generated by the collapse of the first bubble. For example, Nelson and Duda (1982) have shown pressure-time traces generated by the collapse of bubbles generated during the triggered explosions of drops of CO_2 laser-melted iron oxide. In some of their traces, the collapse of large bubbles generated later in the interactions can generate peak pressures larger than those generated by the collapse of smaller bubbles formed earlier in the interactions. Nelson and Duda (1982) observed that drops of CO_2 laser-melted iron oxide never generated hydrogen by the melt-water reaction either before or during the triggered explosions.

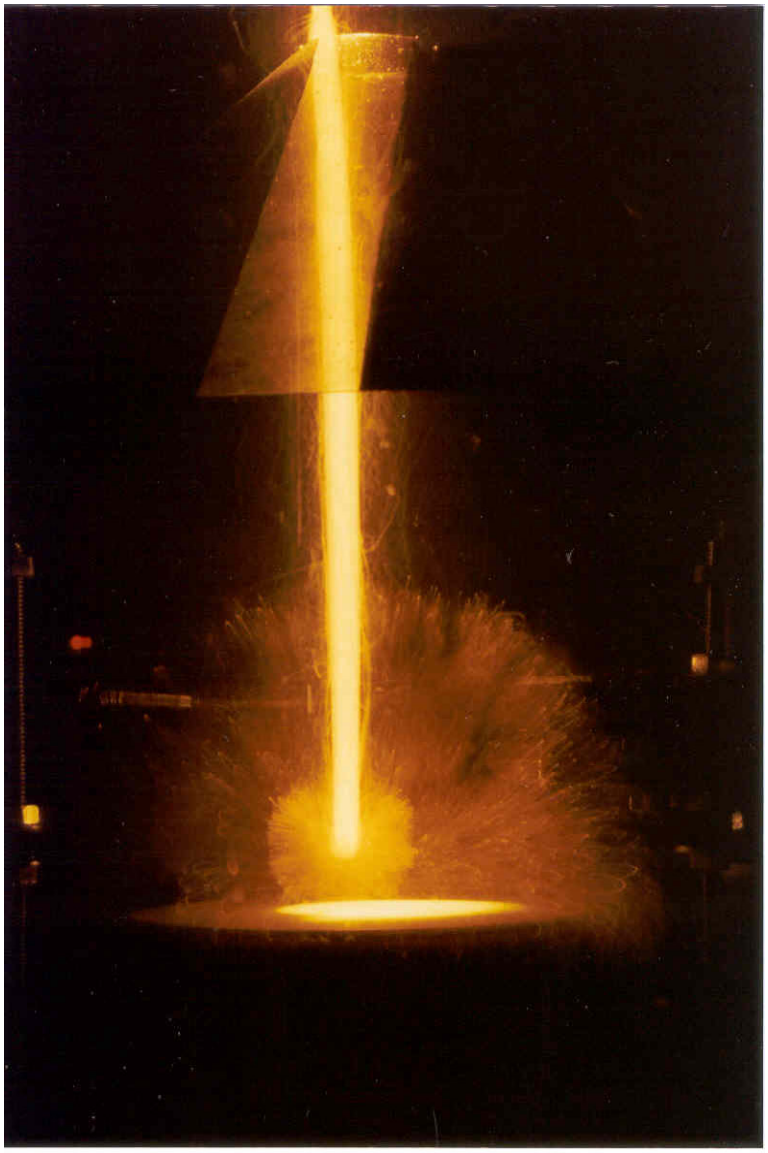

Figure 12. Time-exposed photograph of a drop of molten silicon alloyed with 0.51 wt. % aluminum. Note the smaller bright, spherical image of the bubble that generates the strong pressure transient PT 3 when it collapses. (D-217-1-4)

Comparisons of Pressure-Time Traces

At least 100 pressure-time traces with 32,768 data points each have been recorded and saved to floppy disk during 1999 and 2000. Because of their large number and complexity, we are able to discuss briefly and compare only a few of these traces in this report.

Effect of Alloying Silicon on the Pressure-Time Traces

During this year, we reexamined the effects of alloying the silicon rods from which the drops are prepared on the triggered interactions. Three new experiments were performed with drops of molten silicon that had been alloyed with small amounts of Al and/or Ca with the compositions shown in Table 2 (see also Table A-1 in Appendix A); the results are summarized in Table 5. This new set of experiments essentially repeats similar experiments performed during 1999 (Table 1C of Nelson et al., 2000), but with the addition of making pressure-time measurements during the triggered interactions.

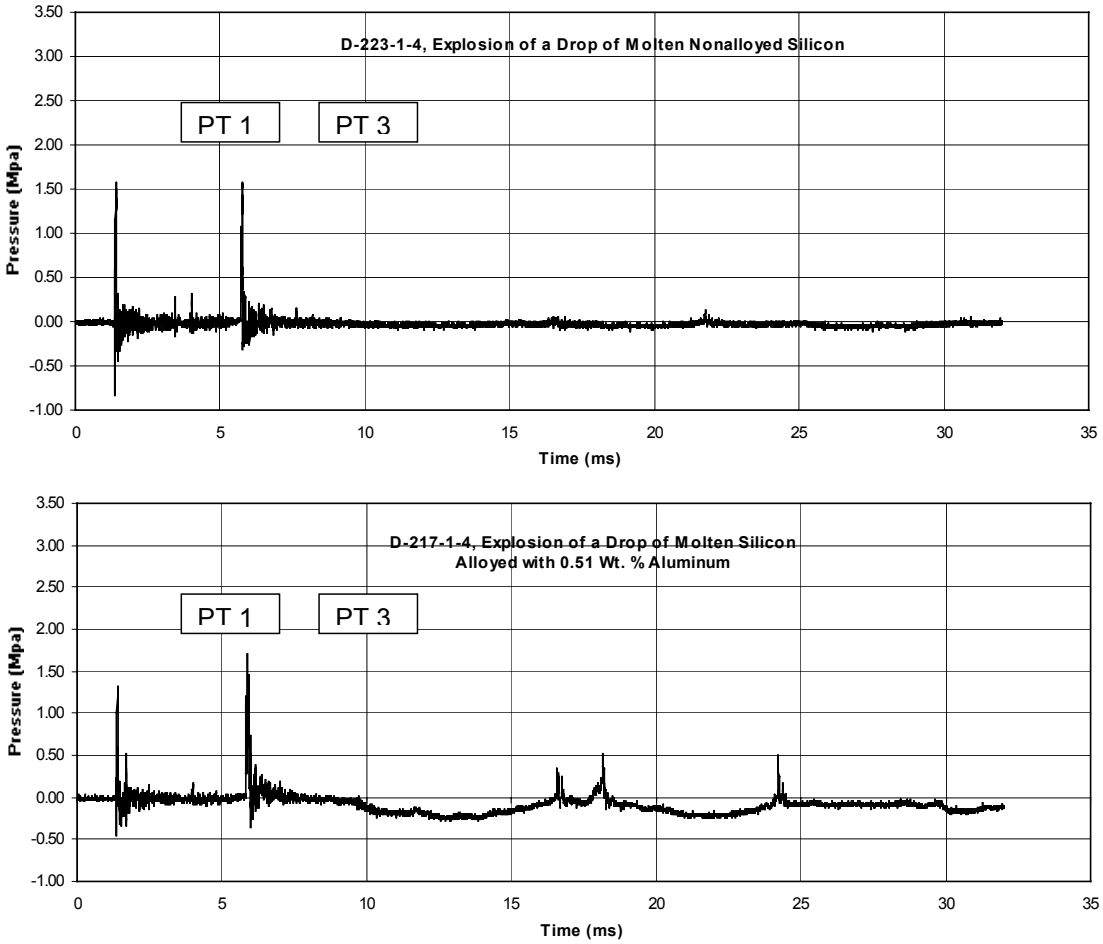

Figure 13. Comparison of pressure-time traces generated during the explosion of a drop of nonalloyed silicon (above) and of a drop alloyed with 0.51 wt. % aluminum (below). Triggering conditions were essentially identical.

The results obtained in 2000 were similar to those obtained in 1999. The drops prepared from alloys that contained calcium (Batches C (Ca additive only) (D-219-1) and D (both Al and Ca additives) (D-221-1)) produced only mild interactions with coarse fragmentation of the melt. The pressure-time traces recorded during both interactions were essentially the same as the triggering transients generated by the impactor alone.

But the drop prepared from the alloy that contained only the aluminum additive (Batch B (Al additive only) (D-217-1)) produced a very strong explosion that threw a lot of water and disabled our hydrogen collection apparatus (the strength of the explosion was similar to that of experiment D-202-1). The pressure-time trace recorded during this interaction showed a number of strong peaks, a long separation between PT 1 and PT 3 (the time for the first bubble to collapse, see Figure 12), and two 10 to 20 ms-long periods of negative pressurization–rarefactions as large as twice atmospheric pressure. In Figure 13, this unusual pressure-time trace is compared with the trace generated by a drop of nonalloyed silicon (D-223-1) that was triggered

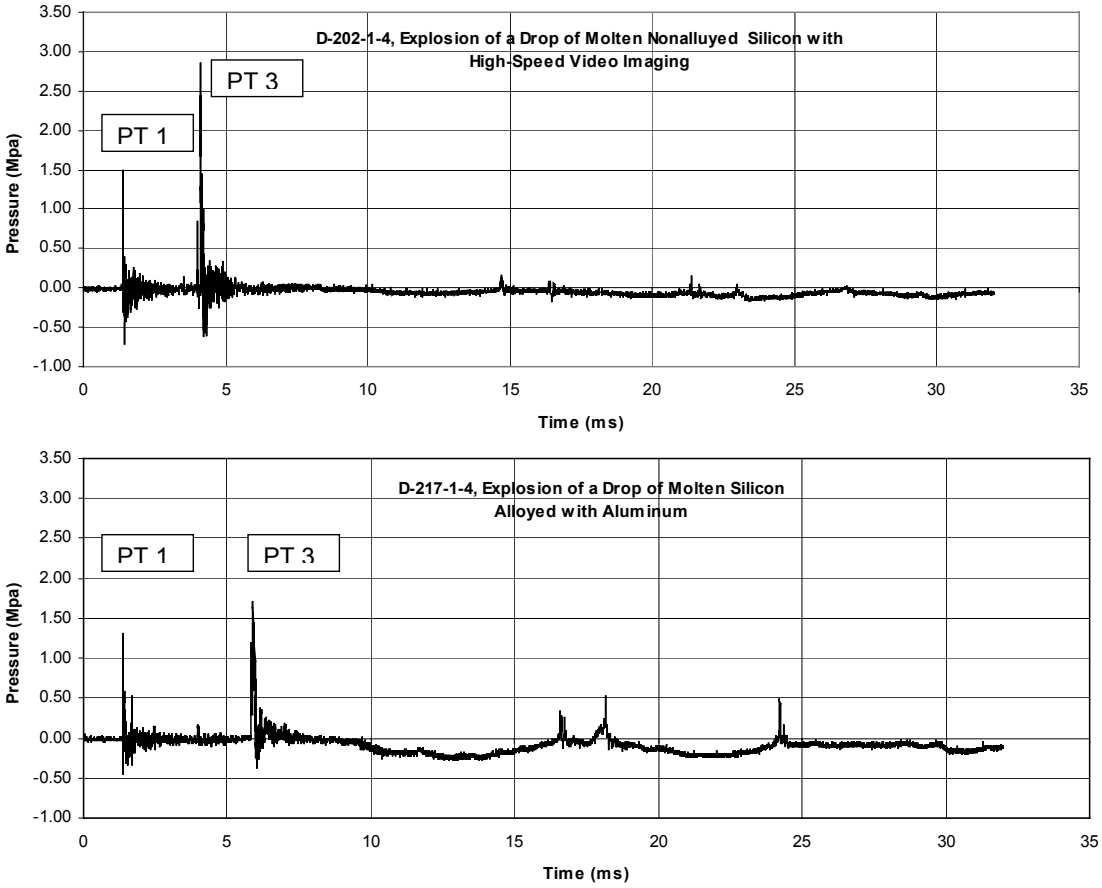

Figure 14. Comparison of pressure-time traces generated during the two strongest explosions: of a drop of nonalloyed silicon (above) and of a drop alloyed with 0.51 wt. % aluminum (below). Triggering depths were 305 mm and 260 mm.

under virtually identical conditions. The nonalloyed drop also produced a strong explosion, but it was not as strong as the explosion produced by the drop with the aluminum additive (D-217-1) (e. g., it did not throw water or disable the hydrogen collector).

Traces Recorded During the Strongest Explosions

Our two strongest explosions were produced in experiments D-202-1-4 (nonalloyed silicon) and D-217-1-4 (silicon alloyed with Al). Both were very vigorous, threw water and disabled the hydrogen collector. Although the effects produced by these explosions seemed similar, their pressure traces differed considerably. These traces are compared in Figure 14.

Several differences between the traces are apparent:

a. The peak pressure produced by the explosion is much greater for the nonalloyed silicon than for the silicon alloyed with Al.

b. The time interval between the major pressure transients, PT 1 and PT 3, is shorter for the nonalloyed silicon than for the silicon alloyed with Al.

c. The time interval between the triggering transient, PT 1, and the minor pressure transients, those later than about 10 ms, is likewise shorter for the nonalloyed silicon than for the silicon alloyed with Al.

d. The minor pressure transients, those later than about 10 ms, are significantly stronger for the silicon alloyed with Al than for the nonalloyed silicon.

e. The rarefactions produced during the explosion of the silicon alloyed with Al are absent during the explosion of the nonalloyed silicon.

And related to the strongest explosion of a drop of nonalloyed silicon, comparison of Figures 13 and 14 shows that:

f. The time interval between the major pressure transients, PT 1 and PT 3, in two similar explosions of drops of nonalloyed silicon seems to change significantly with only minor differences in triggering; thus, the separation between these peaks decreases from 4.374 ms in experiment D-223-1-4 to 2.732 ms in experiment D-202-1-4 as the triggering depth is increased from 260 mm to 305 mm.

Unfortunately, it is not possible to discuss these observations or to analyze, interpret and explain the many other pressure-time traces more thoroughly at this time.

CONCLUSIONS

The experiments performed during the year 2000 were directed toward interpreting and understanding pressure-time records generated during triggered steam explosions of single drops of molten silicon and ferrosilicon. These experiments extend the observations of pressurizations produced when a single drop of molten silicon exploded in experiment D-150-1 (Nelson et al., 2000).

In this final report, after discussing experimental improvements and the characterization of Impactor 3, we describe new experiments performed with single drops of the molten ferrosilicon alloy that contains 75 wt. % silicon and 25 wt. % iron (FeSi75) and drops of silicon, both nonalloyed and containing small amounts of Al and/or Ca additives.

These experiments produced important new information about the triggered steam explosions of drops of these molten metals. This knowledge has resulted primarily from the new instrumentation made available to our program during year 2000:

- The transducer-oscilloscope pressure measuring system;
- The high-speed video system; and
- The hydrogen collection and measuring system.

Of greatest importance has been the ability to correlate individual video images exactly in time with various characteristics of the pressure-time traces.

APPENDICES

Information related to the work performed in 2000 is included in several appendices as follows: Appendix A, Analyses of Alloyed Silicon Rods; Appendix B, Use of Small Underwater Stoichiometric $H_2 + O_2$ Detonations to Trigger Steam Explosions of Single Drops of a Molten Ferrosilicon Alloy; Appendix C, INFACON 9; and Appendix D, Synopsis of Presentations, Reports and Articles Prepared for SINTEF Materials Technology, Trondheim, Norway, by the Department of Engineering Physics, University of Wisconsin-Madison.

FINAL NOTES

This document originally was submitted to the sponsor, SINTEF Materials Technology, Trondheim, Norway, on March 15, 2001, as the draft final report that describes the research performed at the University of Wisconsin-Madison during 2000. Two informal letter reports that describe this work also have been submitted to the sponsor on October 1, 2000 (Nelson et al., 2000a), and on January 21, 2001 (Nelson et al., 2001).

Related research has been performed at NTNU, the Norwegian Technological University, Trondheim, Norway, under the direction of Professor Johan Kr. Tuset, and has been described in the thesis "Steam explosions during granulation of Si-rich alloys: Effect of Ca- and Al-additions" by Kjetil Hildal, dated 25 March, 2002. It may be accessed via the Internet link http://www.ub.ntnu.no/dravh/000057.pdf.

REFERENCES

Nelson, L. S., and Duda, P. M., 1982, "Steam Explosion Experiments with Single Drops of Iron Oxide Melted with a CO_2 Laser," High Temperatures-High Pressures, 14, 259-281 (1982).

Nelson, L. S., Brooks, P.W., Bonazza, R., and Corradini, M. L., 1998, Steam Explosions of Molten Ferrosilicon Drops Released into Water: Effects of Triggering, Alloying and Water Temperature, Final Report (Draft) Submitted to SINTEF Materials Technology 15 March 1998.

Nelson, L. S., Brooks, P. W., Bonazza, R., Corradini, M. L., and Hildal, K., 1999a, Triggered Steam Explosions of Molten Ferrosilicon Drops: Behavior of Solenoid-Driven and Pneumatic Impactors; Ability to Trigger the Explosions at Various Water Depths; Energetics of the Explosions; Fall Histories; Colloidal Material Deposited During the Explosions, Final Report (Draft), March 15, 1999.

Nelson, L. S., Brooks, P. W., Bonazza, R., and Corradini, M. L., 1999b, "Triggering Steam Explosions of Single Drops of a Molten Ferrosilicon Alloy with a Simple Encapsulated Mechanical Impactor," Metallurgical and Materials Transactions B, 30B, 1083-1088, December, 1999.

Nelson, L. S., Brooks, P. W., Bonazza, R., Corradini, M. L., and Hildal, K., 2000, The Quenching and Steam Explosions of Drops of Molten Silicon Released into Water, Final Report (Draft), March 15, 2000.

Nelson, L. S., Brooks, P. W., Bonazza, R., Corradini, M. L., and Hildal, K., 2000a, The Release of Drops of Molten Ferrosilicon into Water: Pressure Transients Generated During Steam Explosions, Informal Letter Report to SINTEF Materials Technology, Trondheim, Norway, Submitted October 2, 2000.

Nelson, L. S., Brooks, P. W., Bonazza, R., Corradini, M. L., and Hildal, K., 2001, The Release of Drops of Molten Ferrosilicon into Water: Pressure Transients Generated During Steam Explosions, Informal Letter Report to SINTEF Materials Technology, Trondheim, Norway, Submitted January 21, 2001.

APPENDIX A

Analyses of Alloyed Silicon Rods

The alloyed silicon rods supplied by SINTEF Materials Technology, Trondheim, Norway, and used in the experiments at the Department of Engineering Physics University of Wisconsin-Madison during 1999 and 2000 were analyzed by Lilleby Metall, Trondheim, Norway. The results shown in Table A-1 were obtained.

Table A-1. Analyses of Alloyed Silicon Rods

Weight % / Batch	B	C	D
% Fe	0.028	0.033	0.032
% Ca	0.011	0.043	0.032
% Al	0.51	0.064	0.57
% C			
% V	<0.001	<0.001	<0.001
% Cr	<0.001	<0.001	<0.001
% Ni	<0.001	<0.001	<0.001
% Cu	<0.001	<0.001	<0.001
% Mo	0.001	0.002	0.002
% Ti	0.005	0.006	0.005
% Mn	0.001	0.001	0.001
% Mg	0.002	0.002	0.002
% Co	0.003	0.002	0.002
% Zn	0.002	0.001	0.001
% Zr	0.001	0.001	0.001
% Pb	0.001	0.001	0.001
% Sn	0.001	<0.001	<0.001

APPENDIX B

Use of Small Underwater Stoichiometric $H_2 + O_2$ Detonations to Trigger Steam Explosions of Single Drops of a Molten Ferrosilicon Alloy

Stoichiometric Hydrogen-Oxygen Explosions

In 1997, we developed a simple and inexpensive way to produce pressure transients for initiating steam explosions of single drops of molten materials. This technique is chemically driven, involving the underwater detonation of 100 ml of a stoichiometric mixture of gaseous hydrogen and oxygen at local atmospheric pressure a short distance below the drop of melt as it falls through the water. The detonation produces a pressure transient that very effectively initiates the steam explosion of the falling drop. We believe the pressure disturbances and water motion produced by the hydrogen-oxygen detonation destabilize the boiling film that surrounds the falling drops of molten material and thus induce the steam explosions.

The detonation tube, filling tubes and ignition circuit are shown in Figure B-1. The equipment and its operation have been described in the Final Report for 1997 (Nelson et al., 1998).

Transducer Measurements

Although we had used the detonation tube empirically many times for triggering steam explosions, it was only recently that the transducer-oscilloscope capability became available. This instrumentation permits us to quantitatively determine the magnitudes and repeatability of the pressure transients generated by the hydrogen-oxygen combustion reactions.

We performed six separate ignition experiments with the pressure measuring equipment, each with the top of the tube about 350 mm below the water surface and the transducer about 100 mm above it. In each experiment, we used fresh fillings of gas, new membranes and new copper filaments. When the gaseous mixtures were ignited, two of the six combustions produced only mild deflagrations, each accompanied by a gentle "pop." The pressurizations were not adequate to trigger the oscilloscope with a minimum triggering level of 0.5 MPa. But in each of the other four combustions, the sound emitted was a sharp "crack," indicating that a detonation had occurred. One of the pressure-time traces recorded during a detonation is reproduced in Figure B-2. For the detonations, a strong initial pressure pulse (PT 1) was recorded by the oscilloscope, followed by several secondary pulses of various heights (PT 2, PT 3, etc.) that were between 5 ms and 10 ms apart. Characteristics of the four detonations are summarized in Table B-1. As shown in this table, the average height of the initial pulses (PT 1's), normalized to 100 mm, was 0.829 ± 0.110 MPa (±13%). (This value should be compared with the pulse height of 0.129 ± 0.0.0239 MPa (±18%) generated by the solenoid-driven impactor (Nelson et al., 1999) and 1.717 ± 0.04377 (±3%), generated by Impactor 3 (Nelson et al., 2000) with both values also normalized to 100 mm.) We attribute the secondary pulses (PT 2, PT 3, etc.) to the collapse of bubbles generated during the combustions.

Initiation of Steam Explosions

To trigger a steam explosion, the detonation tube was placed in the path of a drop of the molten ferrosilicon alloy as it fell through the water. By positioning the tube at a proper depth in the water and choosing an appropriate delay time, the gaseous explosion could be initiated when the falling drop was a short distance above the tube. A time-exposed photograph of an explosion triggered this way is shown in Figure B-3. This photograph, taken in a darkened room, records the luminosity emitted by the hot, molten material, first as the linear vertical image of the intact drop as it falls through the water, and then as the spherical spray of fine particles produced in the explosion. Also, in the lower portion of this photograph, the luminosity emitted by the hydrogen-oxygen detonation can be seen, including a greenish component toward the bottom of the tube attributed to the explosion of the copper filament.

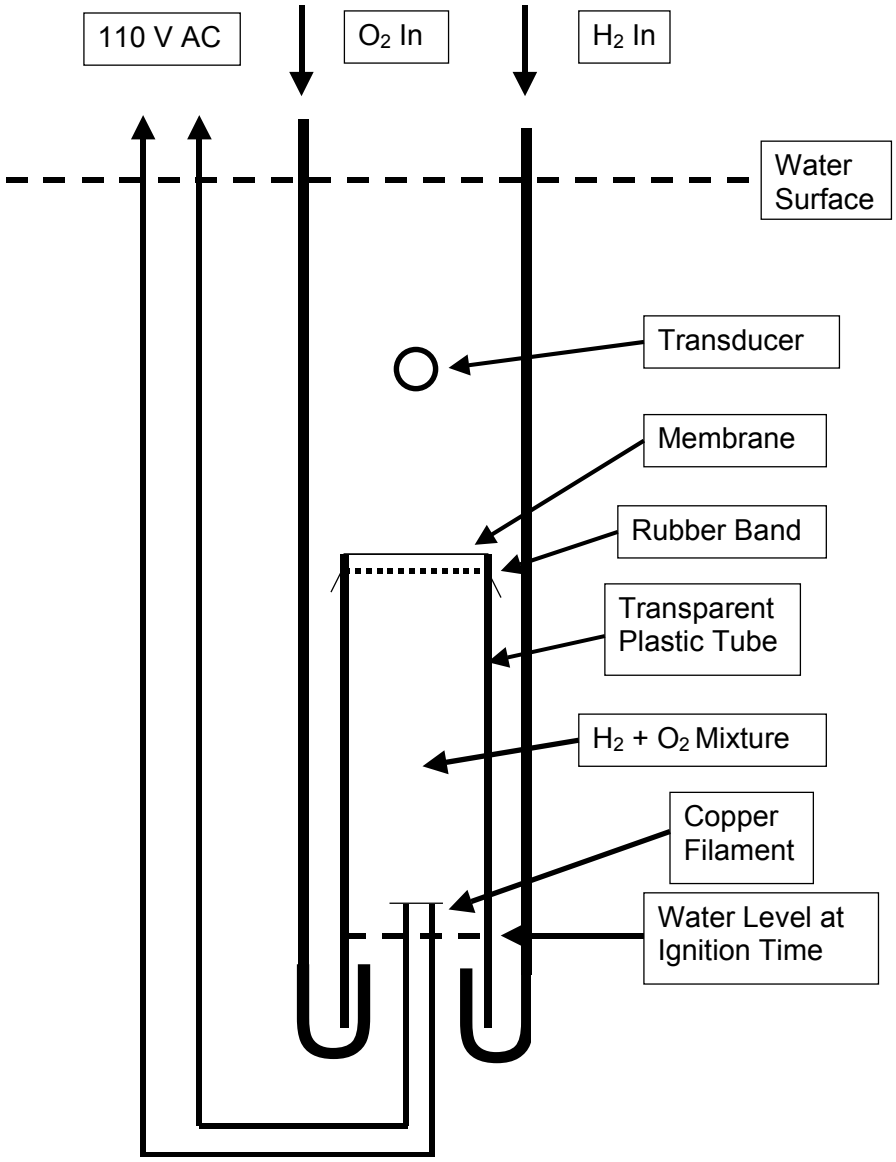

Figure B- 1. Schematic of the detonation tube, filling tubes and ignition circuit.

By scaling the image in Figure B-3 against known distances in the chamber, we determined that the true separation between the drop and the top of the combustion tube at the time of explosion was 72 mm. Then, using the 1/r relationship and the average maximum pressure of PT 1 of 0.829 MPa at 100 mm obtained from Table B-1, we estimated that the explosion was triggered with a pressure transient of 1.2 MPa with an uncertainty of about ±13%. This value far exceeds the threshold value of 0.3 MPa, generated about 43 mm above the solenoid-driven impactor, required to trigger a 9 mm-diameter drop of the molten ferrosilicon alloy, as reported earlier (Nelson et al. 1999).

Paper Submitted to Combustion Science and Technology

On October 5, 2000, we submitted the manuscript titled "Use of Small Underwater Stoichiometric H_2 + O_2 Detonations to Trigger Steam Explosions of Single Drops of a Molten Ferrosilicon Alloy" by Lloyd S.

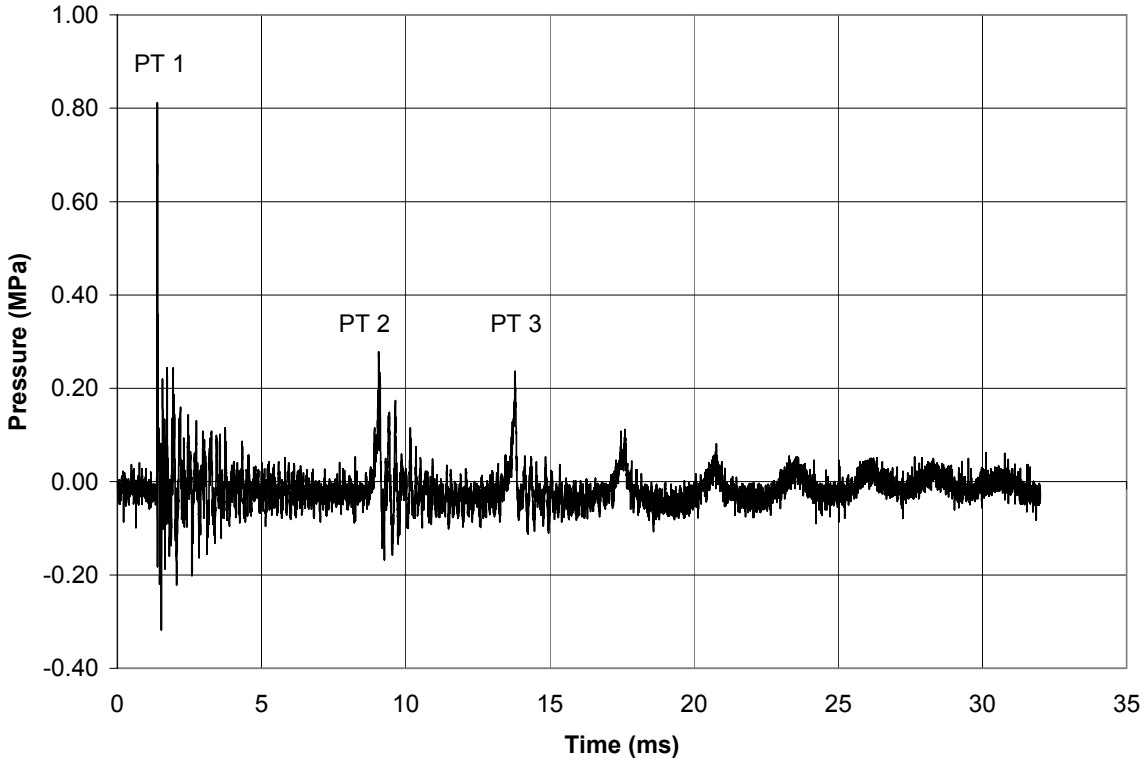

Figure B-2. Pressure-time trace recorded above the underwater detonation of 100 ml of a stoichiometric hydrogen-oxygen mixture at atmospheric pressure. Trace has been normalized to a distance of 100 mm. (D-212-3).

Nelson, Paul W. Brooks, Riccardo Bonazza, Michael L. Corradini and Kjetil Hildal to be considered for publication in the journal Combustion Science and Technology.

References for Appendix B

L. S. Nelson, P. W. Brooks, R. Bonazza and M. L Corradini, 1998, Steam Explosions of Molten Ferrosilicon Drops Released into Water: Effects of Triggering, Alloying and Water Temperature, Final Report (Draft), March 15, 1998.

Nelson, L. S., Brooks, P. W., Bonazza, R., and Corradini, M. L., 1999, "Triggering Steam Explosions of Single Drops of a Molten Ferrosilicon Alloy with a Simple Encapsulated Mechanical Impactor," Metallurgical and Materials Transactions B, 30B, 1083-1088, December 1999.

Nelson, L. S., Brooks, P. W., Bonazza, R., Corradini, M. L., and Hildal, K., 2000, The Quenching and Steam Explosions of Drops of Molten Silicon Released into Water, Final Report (Draft), March 15,2000.

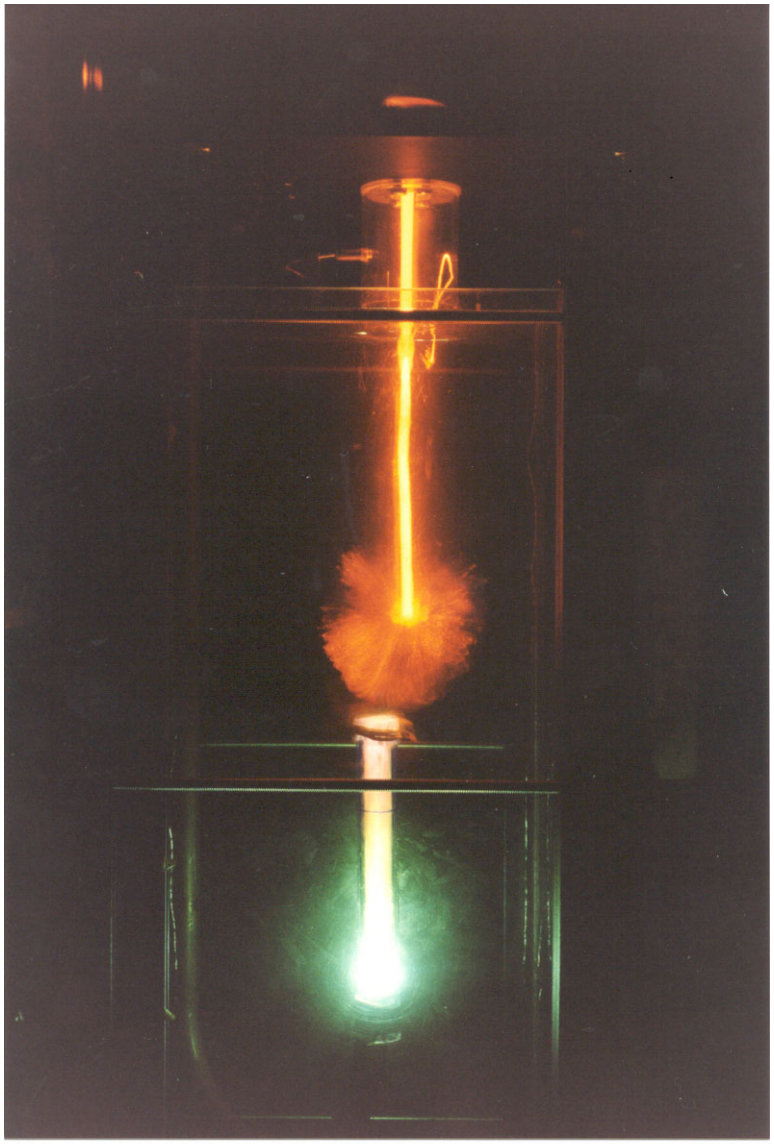

Figure B-3. Time-exposed photograph of the steam explosion of a 9 mm-diameter drop of molten ferrosilicon, (above), initiated by the underwater detonation of 100 ml of a stoichiometric hydrogen-oxygen mixture at atmospheric pressure in the combustion tube (below). Vertical distance between the horizontal crossrods is 324 mm. (C-154-2).

Table B-1. Pressure Transients Generated by the Hydrogen-Oxygen Detonation Tube. Maximum Pressures are Normalized to a Distance of 100 mm.

Trial No.	Transient No.	P(max) (MPa)	Time after PT 1 (ms)
1	PT 1	0.986	0.000
	PT 2	NM	NM
	PT 3	NM	NM
2	PT 1	0.803	0.000
	PT 2	0.276	7.675
	PT 3	0.227	12.405
3	PT 1	0.731	0.000
	PT 2	1.093	7.043
	PT 3	0.149	11.416
4	PT 1	0.796	0.000
	PT 2	1.049	6.761
	PT 3	0.089	10.946
Average PT 1		0.829	
Standard Deviation		0.110	
		±13%	

APPENDIX C

INFACON 9

A paper titled “Steam Explosions of Single Drops of Molten Silicon-Rich Alloys” by Lloyd S. Nelson, Paul W. Brooks, Riccardo Bonazza, Michael L. Corradini, Kjetil Hildal and Trond H. Bergstrøm has been accepted by The Ferroalloys Association, Washington, DC, for publication in the Proceedings of IINFACON 9, Quebec City, June, 2001.

A presentation of the same title will be presented at this conference.

APPENDIX D

Synopsis of Presentations, Reports and Articles Prepared for SINTEF Materials Technology, Trondheim, Norway, by the Department of Engineering Physics, University of Wisconsin-Madison.

1. L.S. Nelson, R. Bonazza and M.L. Corradini; "Formation of 10-20 mm Drops of Molten Ferrosilicon", University of Wisconsin-Madison Report No. UWFDM-1027, June, 1995.

2. Lloyd S. Nelson, Riccardo Bonazza, Paul W. Brooks and Michael L. Corradini; "Quenching 10-20 mm-Diameter Drops of Molten Ferrosilicon in Water and on Solids", Draft, March 1997.

3. Lloyd S. Nelson, "Review of Steam Explosions Emphasizing Single Drops", Seminar at Mo-I-Rana, Norway, April 8, 1997.

4. Lloyd S. Nelson, "Results from Explosion Tests", Seminar at Mo-I-Rana, Norway, April 8, 1997.

5. Lloyd S. Nelson, Paul W. Brooks, Riccardo Bonazza and Michael L. Corradini; "Generation of Pressure Transients for the Initiation of Steam Explosions of Single Drops of Melt", Informal Letter Report (Draft), June 30, 1997.

6. Lloyd S. Nelson, Paul W. Brooks, Riccardo Bonazza and Michael L. Corradini; "Release of Molten Ferrosilicon Drops into Water: Effects of Triggering and Alloying", Informal Letter Report (Draft), September 1, 1997.

7. Lloyd S. Nelson, Paul W. Brooks, Riccardo Bonazza and Michael L. Corradini; "Release of Molten Ferrosilicon Drops into Water: Part 2 Effects of Triggering, Alloying and Water Temperature", Informal Letter Report (Draft), December 31, 1997.

8. Lloyd S. Nelson, Paul W. Brooks, Riccardo Bonazza and Michael L. Corradini; "Generation of Pressure Transients in Water for Triggering Steam Explosions of Single Drops of Melt: A Simple and Inexpensive Mechanical Impactor", Paper intended for publication (Draft), March 11, 1998.

9. Lloyd S. Nelson, Paul W. Brooks, Riccardo Bonazza and Michael Corradini; "Steam Explosions of Molten Ferrosilicon Drops Released into Water: Effects of Triggering, Alloying and Water Temperature", Final Report (Draft), March 15, 1998.

10. Lloyd S. Nelson, Paul W. Brooks, Riccardo Bonazza and Michael L. Corradini; "Release of Molten Ferrosilicon Drops into Water: Effects of Triggering and Alloying", SINTEF/UW Review and Discussions, May 27 and 28, 1998.

11. Lloyd S. Nelson, Paul W. Brooks, Riccardo Bonazza and Michael L. Corradini; "Pressure Transients Generated by Solenoid-Driven and Pneumatic Impactors for Triggering Steam Explosions of Single Drops of Molten Ferrosilicon Alloys", Informal Letter Report (Draft), July 1, 1998.

12. Lloyd S. Nelson, Paul W. Brooks, Riccardo Bonazza and Michael L. Corradini; "A Simple Encapsulated Mechanical Impactor for Triggering Steam Explosions of Single Drops of a Molten Ferrosilicon Alloy", Paper intended for publication (Draft), August 17, 1998.

13. Lloyd S. Nelson, Paul W. Brooks, Riccardo Bonazza, Michael L. Corradini and Kjetil Hildal; "Triggered Steam Explosions of Molten Ferrosilicon Drops: Explosiveness as Water Depth Increases;

Colloidal Material Deposited in the Water During the Explosions", Informal Summary Report (Draft), October 1, 1998.

14. Lloyd S. Nelson, Paul W. Brooks, Riccardo Bonazza, Michael L. Corradini and Kjetil Hildal; Triggered Steam Explosions of Molten Ferrosilicon Drops", Presentation at Ferrolegeringsseminar, Trondheim, Norway, October 21, 1998.

15. Lloyd S. Nelson, Paul W. Brooks, Riccardo Bonazza, Michael L. Corradini and Kjetil Hildal; "Triggered Steam Explosions of Molten Ferrosilicon Drops: Ability to Trigger the Explosions at Various Water Depths; Energetics of the Explosions; Fall Histories; Colloidal Material Deposited During the Explosions", Informal Letter Report (Draft), December 31, 1998.

16. Lloyd S. Nelson, Paul W. Brooks, Riccardo Bonazza and Michael L. Corradini and Kjetil Hildal, "Triggered Steam Explosions of Molten Ferrosilicon Drops: Behavior of Solenoid-Driven and Pneumatic Impactors; Ability to Trigger the Explosions at Various Water Depths; Energetics of the Explosions; Fall Histories; Colloidal Material Deposited During the Explosions," Final Report (Draft), March 15, 1999.

17. Lloyd S. Nelson, Paul W. Brooks, Riccardo Bonazza and Michael L. Corradini, "The Quenching and Steam Explosions of Drops of Molten Silicon Released into Water," Informal Letter Report, [Draft (Revised)], July 1, 1999.

18. Lloyd S. Nelson, Paul W. Brooks, Riccardo Bonazza, Michael L. Corradini and Kjetil Hildal, "The Release of Drops of Molten Silicon into Water: Quenching, Steam Explosions and Hydrogen Generation," Informal Letter Report (Draft), October 1, 1999.

19. Lloyd S. Nelson, Paul W. Brooks, Riccardo Bonazza, Michael L. Corradini, Kjetil Hildal and Trond Bergstrom, "Steam Explosions of Single Drops of a Molten Ferrosilicon Alloy," Paper presented at The Minerals, Metals and Materials Society, Fall 1999 Meeting, November 1, 1999, Cincinnati, Ohio.

20. L. S. Nelson, P. W. Brooks, R. Bonazza and M. L. Corradini, "Triggering Steam Explosions of Single Drops of a Molten Ferrosilicon Alloy with a Simple Encapsulated Mechanical Impactor," Metallurgical and Materials Transactions B, 30B, 1083-1088, December, 1999.

21. Lloyd S. Nelson, Paul W. Brooks, Riccardo Bonazza, Michael L. Corradini and Kjetil Hildal, "The Release of Drops of Molten Silicon into Water: Effects of Alloying; Collection of Hydrogen; Pressure Transients Generated by a Steam Explosion," Informal Letter Report (Draft), January 15, 2000.

22. Lloyd S. Nelson, Paul W. Brooks, Riccardo Bonazza, Michael L. Corradini and Kjetil Hildal, The Quenching and Steam Explosions of Drops of Molten Silicon Released into Water, Final Report (Draft), March 15, 2000.

23. Lloyd S. Nelson, Paul W. Brooks, Riccardo Bonazza, Michael L. Corradini and Kjetil Hildal, The Release of Drops of Molten Ferrosilicon into Water: Pressure Transients Generated During Steam Explosions, Informal Letter Report (Draft), October 2, 2000.

24. Lloyd S. Nelson, Paul W. Brooks, Riccardo Bonazza, Michael L. Corradini and Kjetil Hildal, The Release of Drops of Molten Ferrosilicon and Silicon into Water: Pressure Transients Generated During Steam Explosions, Informal Letter Report (Draft), January 21, 2001.

25. Lloyd S. Nelson, Paul W. Brooks, Riccardo Bonazza, Michael L. Corradini and Kjetil Hildal, The Release of Drops of Molten Ferrosilicon and Silicon into Water: Pressure Transients Generated During Steam Explosions, Final Report (Draft), March 15, 2001.

26. Lloyd S. Nelson, Paul W. Brooks, Riccardo Bonazza, Michael L. Corradini, Kjetil Hildal and Trond H. Bergstrøm, "Steam Explosions of Single Drops of Molten Silicon-Rich Alloys," paper accepted by The Ferroalloys Association, Washington, DC, for presentation at and publication in the Proceedings of IINFACON 9, Quebec City, June, 2001.

27. Lloyd S. Nelson, Paul W. Brooks, Riccardo Bonazza, Michael L. Corradini and Kjetil Hildal, "Use of Small Underwater Stoichiometric $H_2 + O_2$ Detonations to Trigger Steam Explosions of Single Drops of a Molten Ferrosilicon Alloy," manuscript submitted for publication in the journal Combustion Science and Technology, October 5, 2000.